DESY 05-154

Hot QCD, k-strings and the adjoint monopole gas model

Chris P. Korthals Altes
Centre Physique Théorique au CNRS
Case 907, Campus de Luminy, F13288, Marseille, France

Harvey B. Meyer[1]
DESY
Platanenallee 6
D-15738 Zeuthen

Abstract

When the magnetic sector of hot QCD, 3D SU(N) Yang-Mills theory, is described as a dilute gas of non-Abelian monopoles in the adjoint representation of the magnetic group, Wilson loops of $\mathcal{N}$-ality k are known to obey a periodic $k(N-k)$ law. Lattice simulations have confirmed this prediction to a few percent for $N = 4$ and 6. We describe in detail how the magnetic flux of the monopoles produces different area laws for spatial Wilson k-loops. A simple physical argument is presented, why the predicted and observed Casimir scaling is allowed in the large-N limit by usual power-counting arguments. The same scaling is also known to hold in two-loop perturbation theory for the spatial 't Hooft loop, which measures the electric flux. We then present new lattice data for 3D $N = 8$ k-strings as long as 3'fm' that provide further confirmation. Finally we suggest new tests in theories with spontaneous breaking and in $SO(4n+2)$ gauge groups.

[1] harvey.meyer@desy.de

1 Introduction

The title of this paper may sound to most practitioners of lattice gauge theory and hot QCD of a somewhat esoteric nature. And on the other hand aficionados of the beauty of non-Abelian monopoles [3, 4, 6] [8, 5] [7, 10] may reflect on the title as being heretic, since non-Abelian monopoles have so far withstood the traditional approach that has been implemented successfully for 't Hooft-Polyakov monopoles: as yet, nobody has come up with a viable construction of a classical solution, that is then quantized by semi-classical methods. Only recently a construction of non-Abelian fluxes in a low energy field theory version has been accomplished [9]. These are models that relegate the intricacies of non-Abelian monopoles to their high energy sector, and manage to construct explicit non-Abelian *fluxes* in the low energy sector.

Somewhat analogously, we will forget about the intricate nature of individual non-Abelian monopoles and assume that a *gas* of such objects has relatively straightforward properties. That will allow us to compute and interpret in a simple-minded way the average behaviour of magnetic flux loops, that is, spatial Wilson loops [19]. Such spatial loops have been measured in lattice simulations by Teper's group [25, 29] in a wide temperature range, thus showing that the predictions of the model can be tested from first principles.

At temperatures well above the critical T_c, the temporal extent of the system becomes negligible, and we are left with a three-dimensional system. This implies that the tension of the spatial loop at such very high T also bears the interpretation of a three-dimensional string tension, due to a chromo-electric flux tube. In other words, our model is also indirectly a model for confinement in 2+1 dimensional gauge theories.

Generally speaking, in non-Abelian SU(N) gauge theories in three and four dimensions, the chromo-electric flux between two static colour sources arranges itself so as to produce a linearly rising potential. This naturally suggests a flux-tube configuration and leads to the string picture of confinement. While in SU(3) there is only one string tension, that of the string appearing between charges in the fundamental representation, in SU($N \geq 4$) there are $[N/2]$ independent stable 'k-strings' which are protected from screening by the center-symmetry $Z(N)$.

The picture that we propose for the origin of the area laws of the spatial Wilson k-loops, and hence for 3d k-strings, is rooted (perhaps paradoxically) in high temperature 3+1 dimensional QCD and involves a gas of screened non-Abelian monopoles – or rather "magnetic quasi-particles". We prefer the latter terminology, since it stresses that our monopoles need not be eigenstates of the Hamiltonian but are rather collective modes of the plasma. The objects that we shall describe in the 3d gauge theory are the dimensionally reduced versions of these modes, much in the same way as Polyakov's 'pseudoparticles' [14] in the 3d Georgi-Glashow model are the descendants of the t'Hooft-Polyakov monopoles [2] living in the 4d Georgi-Glashow model. The non-Abelian Stokes theorem [49] establishes a connection between spatial Wilson loops and the magnetic flux in the plasma; which in our model is induced by the magnetic quasi-particles. That is, schematically, how we are able to make predictions for 3d k-string tensions.

Of course, k-strings are also interesting in their own right. Since they are perfectly stable, their tension ratios can be used to discriminate unambiguously between models of confinement. In what follows, without giving a comprehensive view of the latter, we put our model in

perspective with respect to a broader class of such models.

Our adjoint monopole gas model [19, 21] is related to the dual-superconductor picture of confinement [1]. The latter would naturally predict the presence of monopoles in the plasma, as manifestations of the condensate at low T. It is a natural generalization of the seminal idea of 't Hooft [16], that Abelian monopoles Bose-condense in the ground state, and are transient states in that they won't show up in the spectrum of the Hamiltonian. In the hot deconfined phase they should populate the ground state, just like gluons. To explain the k-loop tensions in the hot phase is however non-trivial because the number of different species of Abelian monopoles is too small ($N-1$ for SU(N)).

There is the elegant caloron solution to the equations of motion [23]. It is a periodic instanton with a Higgs-like background furnished by the non-trivial value of the Polyakov loop. This gives rise to N monopoles (a fundamental multiplet) inside the caloron. Could these be related to the quasi-particles that we are invoking? It may be [23] that at high enough temperatures the monopoles inside an individual caloron start to "deconfine" and are able to move freely from one to another caloron, much in the same vein that gluons can freely move from one glueball to another at high T. However free monopoles in the fundamental multiplet can *not* explain the observed Casimir scaling [21]. Nevertheless, as explained in the next section, even at asymptotic temperatures we are actually facing *strong* coupling when we try to explain the spatial Wilson loop behaviour. It could well be that this strong coupling favours binding into adjoint monopoles (while binding into singlets is statistically disfavoured at large N). Non-Abelian monopoles in the *adjoint* representation furnish precisely the correct number of species to explain the observed Casimir scaling, as shown in earlier work [19] and in section 4.4 below.

The ratios of k-string tensions are also tests for formulations of SU(N) gauge theories derived from fundamental string theory. Examples of the latter are the MQCD framework [40] and the AdS/CFT calculations in Ref. [42] for $D=3$. The latter give Casimir scaling for N large and k of order N; our model predicts Casimir scaling for any value of N.

The MQCD framework gives a $\sin(k\pi/N)$ law for the k-tension, implying in particular that the tension ratios σ_k/σ_1 have $1/N^2$ corrections. An elegant paper by Gliozzi [22] provides a simple geometric interpretation for the sine law. He shows that in the cold phase the sine law is the borderline between formation of $Z(N)$ symmetric static baryons (no $k \geq 2$ flux tubes involved) and formation of static baryons with $k=2$ or higher flux tubes (it is assumed that arbitrary short flux tubes have the same tension as long flux tubes).

Casimir scaling and the sine law both predict that $\sigma_k/\sigma_1 \to k$ at large N, fixed k; in other words, a k-string is a collection of k non-interacting fundamental strings in the planar limit $N \to \infty$. Casimir scaling however attributes a binding energy to these k strings of order $1/N$, while if the sine law is correct, this energy is only $\mathcal{O}(1/N^2)$. Recently there has been a discussion [39] on the conflict of $1/N$ corrections with standard $1/N$ power-counting rules, based on the assumption that *all* representations with a given $\mathcal{N}$-ality k produce the same tension. We point out in section 6 that this analysis neglects mixing effects between reducible representations which are of order $1/N$ and which lower the energy of the lightest string by an amount of that order. Earlier work on strong coupling expansions [43] corroborates our general argument. More recently, analytic calculations of the tension for 't Hooft loops [20, 19] have

been shown to lead to the same $k(N-k)$ scaling law.

As already mentioned, lattice calculations have been carried out [25, 26, 29] in three and four dimensional SU(N) gauge theory to determine the ratios of the k-string tensions to the fundamental string tension. Here we study the k-strings in 3d SU(N) gauge theories, presenting new data for their tension ratios obtained for the gauge group SU(8) and combining the new information with previously obtained SU(4) and SU(6) data [25]. The numerical advantage of searching for the effect of monopoles on Wilson loops at high T is that the relevant simulations are three-dimensional; needless to say, to obtain the same accuracy, the amount of computational effort is considerably lower for the 3d simulations employing the reduced action.

By the same token, given such an accuracy for the 3d lattice data, it is useful to know to what accuracy in the coupling $g(T)$ the dimensionally reduced actions reproduce the full 4d QCD result. For the case of three colours one knows [38] that the 3d results for the string tension reproduce the 4d lattice data up to $1.1T_c$ through the running of $g(T)$ up to and including two loops.

The lay-out of the paper is as follows. We start with section 2 on how the problem of the residual strong interactions in hot QCD is attacked quantitatively – by dimensional reduction. In section 3 we review briefly non-Abelian monopoles. We then derive in section 4.2 a Stokes type formula for the spatial Wilson loops that permits us to quantify the effect of the putative non-Abelian monopoles in section 4.4. Then follows section 5 on strings in higher representations where our arguments on the $1/N$ counting are exposed, and the lattice calculation is presented in section 6. Finally we compile and discuss the lattice data accumulated so far (section 6.4) and the paper ends with a general conclusion (section 7).

2 High temperature QCD

This section is meant to introduce the reader into the essentialia of hot QCD, and to motivate the model.

At temperatures well above T_c asymptotic freedom drives the running coupling $g(T)$ down to zero. On the other hand the average density of gluons is the Bose-Einstein density $n_{BE}(p/T)$ ($p = |\vec{p}|$ is the momentum of a gluon). Because of this density the coupling in the plasma has to describe stimulated emission and equals

$$g_{st}^2 = g^2 n_{BE}(p/T) = g^2 \frac{1}{\exp p/T - 1}. \tag{1}$$

This leads to a picture of a gluon plasma, where one has to distinguish three scales:

- hard gluons with momentum p of order T, interacting weakly, $g_{st}^2 = \mathcal{O}(g^2)$.
- soft gluons with momentum p of order gT, still interacting weakly $g_{st}^2 = \mathcal{O}(g)$.
- ultra-soft gluons with momentum $p = \mathcal{O}(g^2 T)$, interacting strongly, $g_{st}^2 = \mathcal{O}(1)$.

Thus, in spite of asymptotic freedom, there is a strongly interacting sector left. Strongly interacting because the large population of ultra-soft energy levels pushes the coupling up [13].

Thus, at these length scales, semi-classical methods are unlikely to apply, as we argued in the introduction.

The hard gluons are familiar from the Stefan-Boltzmann form for the pressure. The hard gluons cause Debye screening $m_D \sim gT$ of the force between electric test charges. All this has been known for long from electrodynamic plasmas.

A new feature becomes apparent for the non-Abelian plasma at scales g^2T. It is the screening of the magnetic force ($m_M \sim g^2T$) between two static magnetic test charges. In electrodynamic plasmas no static magnetic screening exists. Magnetic screening not only occurs at arbitrary high temperatures, it *persists* at arbitrary low temperatures, where the electric screening has disappeared and has turned into electric confinement. It is a hallmark of the non-Abelian system, and hints at a magnetic activity for *all* temperatures [12].

One purpose of this paper is to understand and test a specific model [19] for the strongly interacting sector. We will state its assumptions at the end of this section.

2.1 Dimensional reduction at high T

In this section we give a fast review of how one computes equilibrium properties of the plasma in a systematic way. The problem of strong coupling at large distances is dealt with through a sequence of effective actions [35]. It is the last and strongly interacting effective ("magnetic") action that our monopole model approximates.

By integrating out the hard modes in the QCD action one produces an effective 3d action called S_{EQCD}. If one accepts to have an accuracy of $\mathcal{O}(g(T)^4)$ this electrostatic action is the superrenormalizable action in terms of the static potentials. The form of our effective action S_{EQCD} is dictated by all symmetries, global and local, of the original QCD action, which are respected by the integration process. That implies all the symmetries we knew already, except that the electric term in the static action will have no $\partial_0 \vec{A}$ term. So A_0 appears as an adjoint Higgs term in our 3D gauge theory. The electrostatic QCD action density reads:

$$\begin{aligned} \mathcal{L}_E &= \mathrm{Tr}\,\{(\vec{D}(A)A_0)^2\} + m_E^2 \mathrm{Tr}\,\{A_0^2\} + \lambda_E (\mathrm{Tr}\,\{A_0^2\})^2 + \\ &+ \bar{\lambda}_E \left[(\mathrm{Tr}\,\{A_0\})^4 - \frac{1}{2}(\mathrm{Tr}\,\{A_0^2\})^2 \right] + \frac{1}{2}\mathrm{Tr}\,\{F_{ij}^2\} + \delta\mathcal{L}_E. \end{aligned} \tag{2}$$

Because of R- conjugation invariance ($A_0 \to -A_0$) the electrostatic action must be even in A_0. For SU(2) and SU(3) the second quartic term is identically zero.

The parameters in this 3d action are the coupling g_E, the electric mass m_E and the 4-point couplings λ. All of them are expanded in powers of the QCD running coupling $g^2(T)$, and all of them are now known to $\mathcal{O}(g^4)$ [36, 37]. The electric mass coincides with the Debye screening mass $m_D^2 = \frac{g^2 N}{3} T^2$ to one loop order. The 4-point couplings start with the fourth power of $g(T)$. It is customary [45] to express all these parameters in terms of the dimensionful scale g_E, $x = \lambda_E / g_E^2$, similarly for $\bar{x}$, and finally $y = m_E^2 / g_E^4$. For large T the x variable becomes equal to g^2, the xy variable approaches a constant.

In the limit where the electric mass $m_E \sim gT$ becomes very large compared to the coupling $g_E^2 = g^2 T$ one can integrate out this mass scale and obtain magnetic QCD:

$$\mathcal{L}_M = \frac{1}{2}\mathrm{Tr}\,\{F_{ij}^2\} + \delta\mathcal{L}_M. \tag{3}$$

The coupling parameter in this Lagrangian is called g_M and it can be expressed in terms of the electric coupling g_E [48]:

$$g_M^2 = g_E^2 \left[1 - \frac{g_E^2}{16\pi m_E} - \frac{17}{512} \left(\frac{g_E^2}{\pi m_E} \right)^2 \right]. \tag{4}$$

One should realize that in the pure $N = 3$ Yang-mills theory there is only one parameter: the coupling $g(T/\Lambda_T)$. This means there is a relation between x and y, where the physics of the plasma is:

$$xy|_{4D} = \frac{3}{8\pi^2} \left[1 + \frac{3}{2}x + \mathcal{O}(x^2) \right] \quad \text{for} \quad N = 3. \tag{5}$$

This action serves to compute the leading contribution to magnetic quantities like the spatial Wilson loop σ, or the magnetic screening m_M at very high T. For dimensional reasons both are proportional to g_M^2. The corrections are very small, and this seems to be a general feature of this type of corrections [48]. On the other hand the corrections due to hard modes in two loop approximation are appreciable [38]. It turns out that one can extrapolate the 3d result for the Wilson loop to about $1.1T_c$ just by using this 2-loop running of the coupling g_E, as a very good approximation to the 4d results. Quite likely the same is true for the magnetic screening length l_M or magnetic screening mass $m_M = l_M^{-1}$, which is defined from the correlation of a heavy monopole pair: as for the spatial tension, its dominant contribution comes from the 3d magnetic sector.

Summing up: computing magnetic quantities at $T \gg T_c$, in 3d magnetostatic QCD, is sufficient to know them all over the deconfined phase by simply using the two loop running of the coupling. This means that some salient features of our model for the magnetic sector (see next subsection) are valid for all of the deconfined phase.

2.2 Magnetic quasi-particle model for the magnetic sector

The magnetic sector is governed by 3d Yang-Mills theory. For the physics over distances larger than the magnetic screening length we make three Ansaetze:

1. The interaction for the magnetic gluons is so strong that they bind in lumps.
2. The lumps are dilute.
3. The lumps are non-Abelian monopoles.

Their size is on the order of the magnetic screening mass $m_M = \mathcal{O}(g^2 T)$. And so is their inter-particle distance, or their density n_M. The ratio of the two corresponding volumes is the diluteness

$$\delta = n_M / m_M^3. \tag{6}$$

As the coupling drops out in this ratio there is no *parametric* reason that the diluteness is small.

From these Ansaetze follows from simple dilute gas arguments (repeated in section 4.4) that the tension σ of the spatial Wilson loop equals:

$$\sigma \sim \frac{1}{m_M} n_M. \tag{7}$$

There is a group factor in front (which will be discussed in section 4.5), and the the corrections are in powers-not necessarily integer- of the diluteness.

So the diluteness is known, once the tension and the magnetic screening mass are known from lattice measurements. Its smallness is a dynamical effect giving a value of about 0.05 (with a correction of $\mathcal{O}(1/N^2)$ [24]) in the hot phase for SU(N) groups: it is given by the string tension in the 3D gauge theory in units of the lightest glueball mass. Clearly it is gratifying to have an – admittedly empirical – justification for the diluteness being small.

It is instructive to compare our dilute gas of composite lumps with radius l_M to the dilute gas one finds in the usual weak coupling plasmas. There the lumps are point-like particles, and the Debye screening length l_D is *large* with respect to the inter-particle distance, i.e. $l_D^3 n \gg 1$, the weak coupling plasma condition. For hard gluons one has $n \sim T^3$ and $l_D^{-2} \sim g^2$ and the plasma condition is fulfilled.

We want to close this section with a brief comment. It is tempting to go down from infinite temperature to finite temperature, and consider the lumps as magnetic quasiparticles, or collective excitations of the plasma. From our theoretical knowledge of the magnetic screening [31] we know that at $T = 0$ the screening mass equals the lowest glueball mass in the 4D gauge theory; and the spatial Wilson tension equals the string tension at $T = 0$. Lattice simulations [25] find the diluteness at zero temperature, as given by the string tension in units of the lightest glueball mass in the 4D gauge theory, is *still* small, on the order of 0.09 for N large! Thus our dilute gas stays dilute when lowering the temperature. At some temperature T_q the Bose-Einstein statistics takes over (where the ratio of magnetic screening and de Broglie thermal wave length T^{-1} become on the same order). And, in the spirit of dual superconductivity, BE-condensation is then marking the transition to the confined phase.

3 Non-Abelian monopoles

The magnetic sector of hot QCD has magnetic lumps through the strong ($g^2 \sim 1$) binding of magnetic gluons. Very specifically we do not have a Higgs field at our disposal to define the U(1) field strengths. The question is whether other than 't Hooft-Polyakov [2] monopoles can be formed under such circumstances. The answer is not known to date. But if they are there they must obey a Dirac condition.

In 1977, Englert, Windey, Goddard, Olive and Nuyts [3] analysed precisely such hypothetical monopoles in an unbroken gauge theory, and formulated the generalized Dirac condition. This condition is the following. Let B be a matrix in the SU(N) Lie-algebra. Let the colour magnetic field $\vec{B}$ be given far away from the monopole by:

$$\vec{B} = g\vec{r}\frac{B}{4\pi r^3}. \tag{8}$$

The Dirac condition then reads:

$$\exp igB = \mathbf{1}. \tag{9}$$

This condition has to be fulfilled for any matter field that couples to the gauge field. Obviously we can take B to be diagonal. Note also that for U(1) we get the expected result $gB = 2\pi n$.

For any simple Lie group one has the orthogonal set of diagonal generators $\vec{H} = (H_1, \ldots, H_r)$, with r the dimension of the Cartan subalgebra. The remaining orthogonal generators are $E_\alpha = E^\dagger_{-\alpha}$. The roots $\vec{\alpha} = (\alpha_1, \ldots, \alpha_r)$ are given by:

$$\begin{aligned}
[\vec{H}, E_\alpha] &= \vec{\alpha} E_\alpha \\
[E_\alpha, E_\beta] &= (\vec{\alpha} + \vec{\beta}) E_{\alpha+\beta} \quad \text{if } \vec{\alpha} + \vec{\beta} \text{ is a root} \\
[E_\alpha, E_\beta] &= 0 \qquad\qquad\quad \text{otherwise} \\
[E_\alpha, E_{-\alpha}] &= \vec{\alpha} \cdot \vec{H}.
\end{aligned} \tag{10}$$

These definitions imply a common normalization $\mathrm{Tr}\{E_\alpha E_{-\alpha}\} = \mathrm{Tr}\{H_i^2\}$. In physics we are used to have it equal to $1/2$.

We define now the coroots $\vec{\hat{\alpha}} = \frac{\vec{\alpha}}{\vec{\alpha}^2}$. In terms of those the group admits a set of SU(2) subgroups (like the familiar I, U and V spin in SU(3)) for any root α, denoted by $\mathrm{SU}(2)_\alpha$. One gets them by projecting $\vec{H}$ on the coroots and using the E_α. More precisely:

$$\begin{aligned}
\hat{E}_{\pm\alpha} &= \frac{1}{|\vec{\alpha}|} E_{\pm\alpha} \\
\hat{H}_\alpha &= \frac{\vec{\alpha}}{\vec{\alpha}^2} \cdot \vec{H}.
\end{aligned} \tag{11}$$

Crucial is now that the matrices $\hat{H}_\alpha$, being homogeneous in the roots and the H_i, are *independent* of the normalization of the matrices H_i. Hence they have eigenvalues, which are pure numbers. What are those?

The commutation relations that normalize H_α follow from Eq. 10, with the result:

$$[\hat{E}_\alpha, \hat{E}_{-\alpha}] = \hat{H}_\alpha. \tag{12}$$

The weights of an irreducible representation are given by the eigenvalues of the diagonal operators. So if the carrier vectors $v_{(k)}$ diagonalize the representation we can define the weights $\vec{w}_k$ by :

$$\vec{H} v_{(k)} = \vec{w}_k v_{(k)}. \tag{13}$$

Now a theorem on Lie algebras [11] tells us that $2\hat{H}_\alpha$ has integer eigenvalues on any irreducible representation, and hence from Eq. 13:

$$2\frac{\vec{\alpha}}{\vec{\alpha}^2}\vec{w}_k \quad \text{is integer.} \tag{14}$$

So on any irreducible representation the eigenvalues of H_α are (half)- integer. This fact tells us that the magnetic roots $\vec{b}$ defined by

$$B = \frac{4\pi}{g}\vec{b} \cdot \vec{H} \tag{15}$$

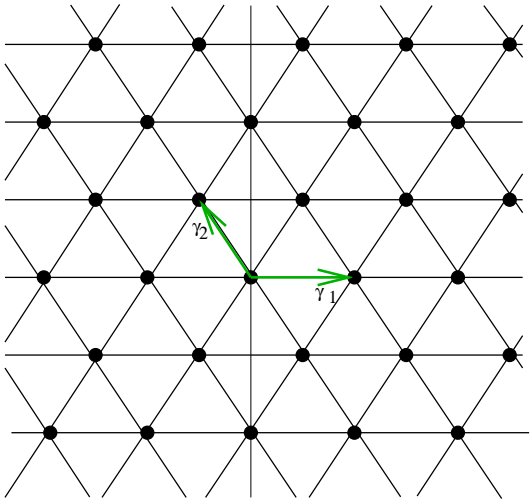

Figure 1: The lattice of allowed magnetic charges spanned by the coroots for the gauge group SU(3).

must lie on a lattice generated by coroots $\vec{b} = \frac{\vec{\alpha}}{\vec{\alpha}^2}$ if the magnetic strength B obeys the Dirac condition, Eq. 9. That is, every point $\vec{b}$ on the magnetic root lattice is a linear combination with integer coefficients of the coroots $\frac{\vec{\alpha}}{\vec{\alpha}^2}$.

In Fig. 1 we show the coroot lattice for SU(3). The two simple roots $\vec{\gamma}_{1,2}$ span the lattice. They define, with $\vec{H}$ in the fundamental representation, the matrices

$$\vec{\gamma}_1 \cdot \vec{H} \equiv H_{12} = \frac{1}{2} \text{ diag}(1, -1, 0) \tag{16}$$

$$\vec{\gamma}_2 \cdot \vec{H} \equiv H_{23} = \frac{1}{2} \text{ diag}(0, 1, -1) \tag{17}$$

which indeed have half-integer eigenvalues and are the third components of I-spin and U-spin respectively. Often it is more convenient to work with these matrices than with the root vectors themselves, as the former are truly simple.

For SU(N), the simple roots are given by the generalization of I and U spin. The general representative is:

$$H_{k,k+1} = \frac{1}{2} \text{diag}(0, 0, ...0, 1, -1, 0, ...). \tag{18}$$

The first non-zero member is on the k-th diagonal entry, and k ranges from 1 to N, with:

$$H_{N,N+1} \equiv H_{N,1} = \frac{1}{2} \text{diag}(-1, 0, ..., 0, 1). \tag{19}$$

The sum of these matrices is zero, and usually the first $N-1$ are taken as simple roots. It is then clear that we can rephrase the Dirac condition as:

$$B = \frac{4\pi}{g}(n_{12}H_{12} + ... + n_{N-1,N}H_{N,N-1}), \tag{20}$$

where the n's are integers[1].

[1]This notation is adapted to our notation for the Wilson loop in later sections.

This classifies the possible monopoles for all simple classical Lie-algebras, as hypothesized in the second paper of reference [3].

For the group SU(2) the consequences of the Dirac condition and this hypothesis are simple. We have a doublet with, in units of $4\pi/g$, $I_3 = \pm 1/2$. Then an iso-triplet with in the same units $I_3 = \pm 1, 0$. For a spin J (half)-integer multiplet we have the same. Our matrix $gB/4\pi$ with the spin 1/2 multiplet of magnetic charges gives only on integer spin electric charge multiplets an integer. So the magnetic group of SO(3) is SU(2). On the other hand the iso-triplet of magnetic charges is compatible with any charge multiplet, half integer or integer, and so the magnetic group of SU(2) is SO(3).

More generally, for the gauge group SU(N) all possible monopoles are multiplets of a magnetic group SU(N)/$Z(N)$. The opposite is also true: the gauge group SU(N)/$Z(N)$ admits monopoles in multiplets of the magnetic group SU(N).

In Fig. 1 the lattice is shown for the gauge group SU(3); for the gauge group SU(3)/$Z(3)$ the lattice of monopoles will include the additional sublattice generated by the triplet representation. This additional sublattice is obtained in a natural way by introducing the 2 hypercharges Y_k, k=1,2. Of course they are not uniquely defined. They generate through exponentiation $\exp(i2\pi Y_k)$ the center-group elements of Z(3). We may for instance choose a set which is at a minimal distance (defined as the trace of the square of the matrix) of the center of the Cartan algebra:

$$\begin{aligned} Y_1 &= \frac{1}{3}\,\mathrm{diag}(2,-1,-1) \\ Y_2 &= \frac{1}{3}\,\mathrm{diag}(1,1,-2). \end{aligned} \tag{21}$$

In terms of the simple root matrices one finds:

$$\begin{aligned} Y_1 &= \frac{2}{3}(2H_{12} + H_{23}) \\ Y_2 &= \frac{2}{3}(3H_{23} + 2H_{12} + H_{31}). \end{aligned} \tag{22}$$

So following in Fig. 1 the steps along the weight lattice to arrive at Y_1 one gets the highest weight of the triplet representation. Similarly Y_2 is the highest weight of the anti-triplet representation. In Appendix B we formulate this relationship for general SU(N) and the generators of its center-group $Z(N)$. Not only are the $N-1$ Y matrices an alternative basis for the Cartan algebra. More important for us, they are a measure for the strength of the Wilson loops needed to observe the monopoles (see section 4.2) .

For any general classical Lie group it is the "dual" group [3] built from the dual Lie algebra [11] that gives the possible multiplets. The precise dual *group* with the appropriate center-group follows from the same considerations as for the SU(N) case: the larger the original, electric, gauge group, the more stringent the Dirac condition becomes and a smaller magnetic group follows. In mathematical terms it is the connectivity of the group and the ensuing Z(N) factors.

In an earlier paper [19] precisely these hypothetical monopoles were identified with our lumps in 3 dimensions. As we supposed the lumps – now monopoles – to be dilute we can

compute their effect on Wilson loops. For SU(N) groups the choice of adjoint representation is unquestionably favoured numerically, as simulated by k-loops for $N = 4,\ 6$ by Teper [25] and for $N = 8$ in this paper.

A comment on the nature of the magnetic group is in order. The monopoles, as bound states of magnetic gluons, will transform inside a multiplet under some perhaps very complicated function of the original vector potentials. So the global magnetic SU(N) group will not coincide with the original global colour group. This ties in with a phenomenon discovered by the authors in Ref. [8]: global colour is not defined on the quantized version of the non-Abelian monopoles, due to the long range nature of the colour magnetic fields of the monopole [2].

3.1 Monopoles as a dilute gas: the broken symmetry case in the Georgi-Glashow model

At this stage it is useful to put our model into a well-known context, the Georgi-Glashow model, with gauge group SU(2) in $D = 3$ with gauge coupling g_3. According to our hypothesis we have a dilute gas of iso-triplet monopoles which describes the behaviour of Wilson loops. Their density is proportional to g_3^6, the only scale before breaking the symmetry. And their screening mass is proportional to g_3^2. Adding an adjoint Higgs scalar with a "heavy" VEV v, i.e. $v \gg g_3$, will give us the broken phase with heavy 't Hooft-Polyakov monopoles:

$$SO(3) \to U(1). \tag{23}$$

This model was studied by semi-classical methods in a seminal paper by Polyakov [14], in the limit that g_3/v is small. In that limit the diluteness of the monopoles is a fact. The Wilson loop tension σ is exponentially small, like the density of the monopoles and the screening mass. The exponent is on the order of $\exp -\gamma v/g_3$, γ some numerical constant. The result for the string tension can be expressed in terms of the density of monopoles n_M and the magnetic screening mass M by combining:

$$\sigma = \frac{g_3^2 M}{2\pi^2}\left[1 - \frac{\pi M}{2g_3^2} + \ldots\right], \quad \text{and} \tag{24}$$

$$n_M = \frac{g_3^2 M^2}{32\pi^2}\left[1 + \mathcal{O}\left(\frac{M}{g_3^2}\right)\right] \tag{25}$$

into

$$\sigma = \frac{16 n_M}{M}\left[1 + \mathcal{O}\left(\frac{M}{g_3^2}\right)\right] \tag{26}$$

The correction to the tension is due to the authors in Ref. [15].

Eqs. 25 and 26 are typical for weak coupling plasmas. The dimensionless ratio of tension over screening is proportional to the number of monopoles inside a sphere of radius the screening length:

$$\frac{\sigma}{M^2} = 16\frac{n_M}{M^3}\left[1 + \mathcal{O}\left(\frac{M}{g_3^2}\right)\right]. \tag{27}$$

[2] In the work by Bais and collaborators [6] an interesting interpretation of the magnetic group is proposed but its discussion falls beyond the scope of this paper.

From Eq. 25, this number is seen to be large:

$$\frac{\sigma}{M^2} = 16\frac{n_M}{M^3} = \frac{g_3^2}{(2\pi^2)M} \gg 1. \tag{28}$$

In our model for the strongly interacting symmetric phase (see Eq. 6 and below), this very same ratio is small! Physically, what happens is that the strong coupling creates a bound state of the original semi-classical monopoles within the magnetic screening radius. And indeed, as stated before, Monte-Carlo simulations in the symmetric phase give for the ratio $\frac{\sigma}{M^2}$ 0.046(2) [24].

3.2 Broken symmetry: SU(3)/Z(3) and higher groups

Our next example is the gauge group SU(3)/$Z(3)$ broken by the adjoint to $U(1)^2$ or to SU(2) $\times$ U(1)/$Z(2)$.

The first case is shown in Fig. 2. Every point represents an 't Hooft-Polyakov monopole in the corresponding SU(2) subgroup, as in Eq. 12. The Dirac condition carries integers which are the topological winding numbers of the Higgs field [6]. So this case does not go beyond what we already knew. As we wil see in the sequel this phase is not realized in simulations, so we will not consider this phase anymore.

Figure 2: The lattice of charges allowed by the quantisation condition, spanned by the simple coroots. In this figure also the direction of the Higgs field Φ_0 in the Cartan subalgebra is indicated. In (a) the stable charges for an arbitrary non-degenerate orientation of the Higgs field are indicated by black dots. In that case the residual gauge group is $U(1) \times U(1)$ and all allowed charges correspond to a winding number. In (b) the Higgs field is degenerate and leaves the non-Abelian group $U(2)$ unbroken. Now only one component of the magnetic charge is the winding number, and in each topological sector only the smallest total charge is conserved. The points symmetric with respect to the Higgs field are conjugate through the unbroken group.

More interesting is the breaking pattern with unbroken group U(2). This model is very often used [10] for investigations for non-Abelian monopoles. For momenta $p \gg v$ the broken phase is perturbative, for momenta much smaller than g_3^2 the coupling becomes strong. We expect screening at those distances, including screening of monopoles.

If we try to construct an 't Hooft-Polyakov monopole in the unbroken SU(2) group along $\vec{\gamma}_1$ in Fig. 2, we will fail because the VEV is lacking in that subgroup. Along the root $\vec{\gamma}_2$ the VEV is non-zero, so along that direction the integers still correspond to a winding number. Similarly along the direction $\vec{\gamma}_1 + \vec{\gamma}_2$, obtained by reflection of $\vec{\gamma}_2$ w.r.t. the direction of the

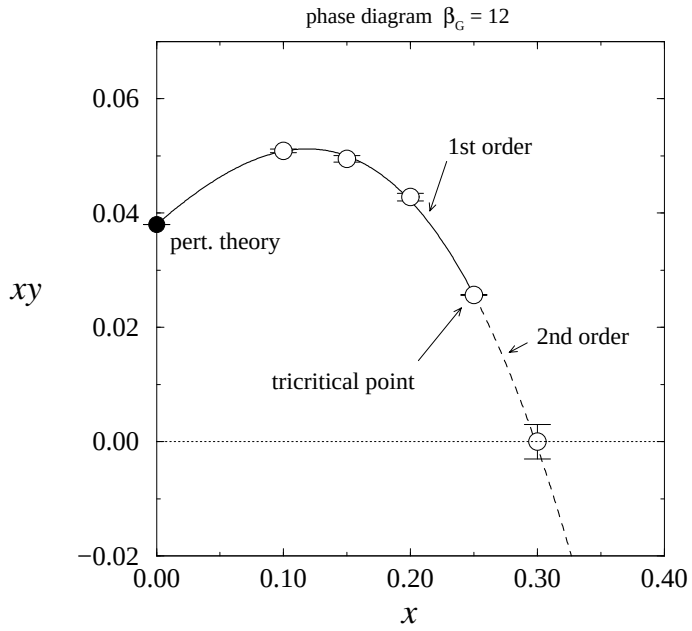

Figure 3: The phase diagram of the 3d SU(3) + adjoint Higgs theory [45]. The open symbols are results from the simulations, and the filled circle is the perturbative result [44, 45].

Higgs breaking Φ_0. Their long range magnetic fields are transforming into each other by the unbroken gauge transformations. When trying to quantize these monopoles this property poses a problem [8] of consistency, which is related to the fact that for the quantized solutions we expect screening. The long range field is unstable.

The mass of these objects is growing with the size of the VEV in the classical approximation. In what follows we will assume that this property survives the non-perturbative quantization. In terms of our model, the dilute gas of light octet monopoles in the symmetric phase will after breaking leave the expected isotriplet in the unbroken SU(2), and two heavy iso-doublets. The iso-triplet stays light after breaking, with a density g_3^6. The iso-doublets are the monopoles we described above and live at the lattice points $\vec{\gamma}_2$ and $\vec{\gamma}_1 + \vec{\gamma}_2$ in Fig. 2. Due to their large mass they have an exponentially small density like the 't Hooft-Polyakov monopoles in the previous example. Note that in both examples the unbroken group defines a neutral singlet, that was present before breaking, but has disappeared in the transition between the two phases.

For illustration we show in Fig. 3 the phase diagram of the electrostatic theory given by the action in Eq. 2 for SU(3) by numerical simulation [45]. The relevant variables are the dimensionless combinations x and xy discussed in section 2.1. There is a first order transition for small x, that is semi-classically calculable [44, 45]. It marks the border of the region where SU(3) symmetry is broken to SU(2) × U(1) and where the global R symmetry is spontaneously broken [44]. For larger x the transition becomes second order. Above the border there is the unbroken phase. This unbroken phase can be smoothly accessed from the broken phase by the dotted, second order transition line. It means that putative monopoles in the unbroken phases are smooth deformations of the monopoles in the broken phase.

Note the absence of a phase where $U(1) \times U(1)$ is unbroken but all other generators are broken [45]. In general, for SU(N), the adjoint Higgs does admit for breakings of the type SU(k) $\times$ SU($N-k$) $\times$ U(1) [46].

This phase diagram not only relates the putative monopoles in the unbroken phase to their more familiar analogues in the broken phase [47]. In order to detect the monopoles one needs an operator that measures their flux. This operator is the Stokes version of the spatial Wilson loop, and is intimately related to a similar operator for the broken phase. This is the subject of the next section.

4 Flux representation for spatial 't Hooft and Wilson loops

The monopoles have an effect on spatial Wilson loops, because the loops record magnetic flux. The traditional representation of the loop as a line integral is not appropriate to quantify the effect, and we have to find a flux representation for the loop. For a loop in the U(1) case we have Stokes' theorem:

$$\exp ig \oint_L d\vec{l} \cdot \vec{A} = \exp ig \int d\vec{S} \cdot \vec{B} \qquad \text{for U(1).} \tag{29}$$

Now the non-Abelian case. For a certain class of irreducible representations of SU(N) one finds a simple and useful generalization of the Abelian case. It is due to Diakonov and Petrov [49]. If R is any one of the fully anti-symmetric irreducible representations given by the one column Young tableau with k entries it has highest weight Y_k (see appendix A; recall the property $\exp(i2\pi Y_k) = e^{i2\pi k/N}$). Then one finds for the Wilson loop $W_R(L)$:

$$\mathrm{Tr}\, \mathcal{P} \exp ig \oint_L d\vec{l} \cdot \vec{A}_R = \int D\Omega \ \exp ig \int d\vec{S} \cdot \mathrm{Tr} \left\{ \Omega Y_k \Omega^\dagger \vec{B} \right\}. \tag{30}$$

The integration is over *regular* gauge transforms Ω.

In this section the physical ideas behind this Stokes law will be expounded. There are many papers [50] concerning its derivation, but we have not seen any exploring the significance of the class of gauge transformations involved, nor the special role played by the fully anti-symmetric irreducible representations. First we will make the Stokes theorem plausible by recalling some known features [41] of colour electric analogue of the spatial Wilson loop: the spatial 't Hooft loop.

4.1 Flux representation of the spatial 't Hooft loop

Colour electric flux is confined inside glueballs. It is only above the critical temperature that it becomes visible through the area law obeyed by the thermal average of the spatial 't Hooft loop.

The 't Hooft loop is defined as a loop of a Dirac vortex, with strength $z_k = e^{i2\pi k/N}$ in the center group. The vortex is created by a gauge transformation Ω_k with a discontinuity z_k,

when circumnavigating the vortex. The locus of the discontinuity is a surface S spanned by the vortex L.

We take the simplest gauge transformation that does have a discontinuity of this type. Gauge transformations are generated by Gauss' operator $\vec{D}\cdot\vec{E}$. If $\theta(S)$ makes a unit jump when going through the surface in the direction of the normal $\vec{n}$, then

$$V_k(L) = \exp i\frac{4\pi}{g}\int d\vec{x}\ \mathrm{Tr}\left\{Y_k(\vec{E}\cdot\vec{D})\theta(S)\right\} \tag{31}$$

has the required discontinuity.

On physical states, only the gradient in the covariant derivative $\vec{D}=\vec{\partial}+ig[\vec{A}$, counts [41]. The gluon charge $gf_{abc}\vec{A}.\vec{E}$ is continuous through the surface. So the spatial 't Hooft loop becomes:

$$V_k(L) = \exp i\frac{4\pi}{g}\int d\vec{S}\cdot\mathrm{Tr}\left\{Y_k\vec{E}\right\} \qquad \text{(on physical states)}. \tag{32}$$

This operator does not look gauge invariant, although on the physical subspace it is. In order to bring it in a manifestly gauge-invariant form, we multiply it on the left with a regular gauge transformation Ω, and on the right with $\Omega^\dagger$; a matrix element of V_k between two physical states is not affected by this operation. After integration over all regular transformations,

$$V_k(L) = \int D\Omega\ \exp i\frac{4\pi}{g}\int d\vec{S}\cdot\mathrm{Tr}\left\{\Omega Y_k\Omega^\dagger\vec{E}\right\} \qquad \text{(on physical states)}. \tag{33}$$

is manifestly gauge-invariant.

It seems plausible to obtain its magnetic analogue by replacing $\vec{E}$ by $\vec{B}$ and the coupling $\alpha\equiv g^2/4\pi$ by α^{-1}. That gives the formula for the Wilson loop, Eq. 30.

4.2 The flux representation for the Wilson loop

The plausibility argument from the preceding section gives a formula which is consistent with the expression given in Ref. [49] for Wilson loop in any representation R, with highest weight H_R. Let Ω be any gauge transformation that is periodic on the loop. Then, with $\vec{\nabla}\Omega^\dagger = (\vec{\partial}-ig\vec{A})\Omega^\dagger$ and $\vec{\nabla}\Omega = \vec{\partial}\Omega + ig\Omega\vec{A}$:

$$W_R(L) = \int D\Omega\ \exp ig\int d\vec{S}\cdot\mathrm{Tr}\left\{[H_R\left(\Omega\vec{B}\Omega^\dagger - \frac{1}{ig}\vec{\nabla}\Omega\times\vec{\nabla}\Omega^\dagger\right)\right\}. \tag{34}$$

This result, proved in Appendix B, differs from that of the plausibility argument through the presence of the second term. This term reduces in the SU(2) case to the familiar 't Hooft source term. If we limit ourselves to regular gauge transformations, this second term would drop out in the equations of motion.

In the light of this we feel it is justified to make the following *assumption*: in our model with a dilute monopole gas the contribution of the second term is negligible. A second simplification occurs when we are only interested in its (thermal) expectation value. This is because in this case W_R acts on the left and on the right only on physical states , so the effect of the regular gauge transforms Ω is undone.

There is a further comment related to this Stokes formula . It is derived under the assumption (see Appendix B) that it is regulated by the SU(N) asymmetric top [49]. The question is whether the pure Yang-Mills theory average can be provided with such a regulator. For $N = 2$ and in three dimensions the answer is affirmative [41] by adding an adjoint Higgs system and letting the VEV go to zero, followed by decoupling the Higgs in the infinite mass limit. The VEV is the moment of inertia of the *symmetric* top. We can *not* accommodate the extra parameter of the asymmetric top, and this is the reason that the Stokes formula is then only valid for the fully antisymmetric irreducible representations with highest weight $H_R = Y_k$. The reason for this is that the second order Casimir operator takes its minimal value – with fixed N-ality k – in the fully antisymmetric representation.

For general N the answer is analogous, but Nature realizes only a limited set of Higgs phases with only one adjoint Higgs field. They are limited to breakings of the type where $\mathrm{SU}(k) \times \mathrm{SU}(N-k) \times \mathrm{U}(1)$ is still unbroken, $k \leq [N/2]$ [46]. That implies once more that the proof of the Stokes formula is only valid for those highest weights that have this symmetry, i.e. of the form $H_R = lY_k$, l a positive integer. For $l = 1$ this is the weight of the totally antisymmetric Young tableaux with k boxes. Appendix B shows that $l > 1$ is excluded. This ends our discussion of Eq. 30.

4.3 Electric flux loop and its expectation value

Let us return to the electric flux loop, Eq. 32. In this case the Ω integration drops out when one acts with $V_k(L)$ on a physical state, because the only effect of $V_k(L)$ is to multiply intersecting Wilson loops in the physical state with a center-group factor (see [41] for more details):

$$\exp(i2\pi\Omega Y_k\Omega^\dagger) = \Omega \ \exp(i2\pi Y_k)\ \Omega^\dagger = \exp(ik2\pi/N). \tag{35}$$

The thermal expectation value of the 't Hooft loop has been calculated analytically at high temperature in powers of $g(T)$, including $g(T)^3$. This is possible because the effective potential is in low orders built up by hard modes (O(T)) and soft modes (O(gT)). The ultrasoft magnetic modes come in at higher orders. This potential has a $Z(N)$ symmetry, and the thermal expectation value of the loop tension,

$$\langle V_k(L)\rangle = \exp\left(-\rho_k(T)A(L)\right), \tag{36}$$

is obtained from the tunneling between two vacua, one corresponding to $k = 0$ and one corresponding to k. One finds then [20] that:

$$\rho_k(T) = \rho_1(T)\frac{k(N-k)}{(N-1)}, \tag{37}$$

up and including two loop order. Concretely, in one loop order the value of $\rho_1(T)$ is [18]:

$$\rho_1(T) = \frac{4\pi^2}{3\sqrt{3g^2N}}(N-1)T^2. \tag{38}$$

In three loop the above Casimir scaling is slightly invalidated, as it is found to be in lattice simulations [27, 28].

4.4 Dilute gas approximation for both electric and magnetic flux loops

From the formulae in the preceding subsection one can easily find the behaviour of the tensions in terms of k, once one assumes a dilute gas of gluons for the electric loop and a dilute gas of monopoles for the magnetic loop at high temperature. A dilute gas of gluons at high temperature will certainly disorder the electric loop. The reason is that the flux from one single species of gluons is going through the loop only when within screening distance l_E from the loop:

$$l_E \equiv \frac{1}{m_D} = \sqrt{\frac{3}{g^2 N}}\ \frac{1}{T}. \tag{39}$$

Thus all the flux through the loop can only come from the gluon being in a slab of thickness l_E and area $A(L)$ of the loop. Thus the flux is approximated by a theta-function in the distance d from the loop.

The total flux from a charged gluon is ± 1, as follows from the adjoint representation of Y_k. Thus the height of the theta-function is $\pm\frac{1}{2}$, because half of the flux is lost on the loop. Its effect on the loop is that it picks up a factor

$$V_k(L) = \exp\left[i2\pi\left(\pm\frac{1}{2}\right)\right] = -1. \tag{40}$$

Note that not the value of the charge, but only the multiplicity of the charge depends on k. This multiplicity is $k(N-k)$ for each value.

Now the distribution function of say ℓ gluons of a given charged species in such a slab is peaked around $\bar{\ell}$, the mean number of gluons in the box. Its width should, according to thermodynamics, be proportional to $\bar{\ell}$, like e.g. the Poisson distribution:

$$P(\ell) = \frac{e^{-\bar{\ell}}}{\ell!}(\bar{\ell})^{\ell}. \tag{41}$$

The average of the loop is therefore:

$$\langle V_k(L)\rangle|_{\text{one species}} = \sum_{\ell} P(\ell)(-1)^{\ell} = e^{-2\bar{\ell}}. \tag{42}$$

Together with Eq. 36 this means that a single charged gluon species will determine the thermal average of the loop to be an area law:

$$A(L)\rho_k|_{\text{one species}} = 2\bar{\ell} = 2A(L)l_E\ n(T). \tag{43}$$

Note the absence of k dependence in the outcome! What counts is that the charge is non-zero, but its sign is irrelevant[3].

[3]The reader might be alarmed by our cavalier treatment of the screening of the flux. The flux $\Phi(d)$ that a gluon at distance d shines through the loop is exponential in d, not a theta-function! One can correct for this by dividing the space above and below the loop in parallel slabs of infinitesimal thickness. This means the summand in Eq. 42 is replaced by an integral $\int d(d)\exp[1-\cos\{2\pi\Phi(d)\}]$. As a result the factor 2 in Eq. 43 increases by a factor 1.64282....

Thus the only way the k dependence comes in is when we take all the charged gluons into account. This number, the multiplicity with respect to the charge Y_k, is for the adjoint gluon multiplet equal to $2k(N-k)$. It is the number of non-zero entries in the diagonal adjoint representation of Y_k. We supposed the gluons to be independent; it follows that

$$\rho_k|_{\text{all species}} = 2\bar{\ell} \cdot 2k(N-k) = 4l_E\ n(T)\ k(N-k). \tag{44}$$

Thus the k-loop is proportional to the multiplicity of charged gluons with respect to the charge Y_k. Note also that equation 39, together with the density of the gluons being $\sim T^3$, makes the outcome of the one species calculation parametrically identical to the analytic result in Eq. 38.

The calculation of the magnetic loop is identical. The unit of magnetic charge is $4\pi/g$ instead of g, but this is canceled by changing from electric to magnetic loop. It is useful to realize that the surface integral $\int d\vec{S} \cdot \vec{B}$ for a single magnetic quasiparticle is given by $\frac{1}{2}B$, where B is the magnetic charge matrix satisfying the Dirac condition (see section 3); this condition thus directly leads to the phase π necessary to disorder the Wilson loop, for any member of the adjoint representation. So the thermal expectation for the magnetic k-tension is, as for its electric counterpart:

$$\sigma_k \sim l_M n_M(T)\ k(N-k). \tag{45}$$

Though superficially very alike, there is an important difference between the two tensions in units of the respective screening lengths. The electric tension in those units becomes

$$l_E^2 \rho_k \sim l_E^3 n. \tag{46}$$

On the right hand side we have a large number, $\mathcal{O}(g^{-3}(T))$, for high T. This is the plasma condition. It says that an electric screening volume contains a large number of almost free gluons. And corrections are in terms of inverse fractional powers of this ratio, as discussed already in section 3.1. On the other hand the Wilson k-tension equals:

$$l_M^2 \sigma_k \sim l_M^3 n_M. \tag{47}$$

Both the magnetic screening and the magnetic density are $\mathcal{O}(g^2 T)$. So in the ratio the coupling drops out. Lattice data tell us the l.h.s. is small for all N. The corrections are discussed in section 4.6.

For large N the dimensionless quantity $n_M l_M^3$ is of order $1/N$. This is so because the magnetic screening length l_M can be shown to be given by the 0^{++} mass of the Hamiltonian of 2+1 dimensional Yang-Mills theory, and therefore behaves parametrically like $1/g^2 NT$. The density of a single monopole species n_M should be $\frac{1}{N}(g^2 NT)^3$, in order to recover a tension of $\mathcal{O}(1)$.

4.5 Monopole multiplets other than the adjoint

Now we use a general multiplet R carrying a unitary representation $D_R$of the magnetic group as the magnetic quasi-particles in our model [21]. Its dimension is d_R. The Lie- representative

of the charge Y_k is written as $(Y_k)_R$ and the corresponding group element as $D_R(Y_k)$. Of course $D_R(Y_k) = \exp i(Y_k)_R$

As in the previous subsection, the quasi-particle model produces for a given member r ($r = 1, 2, \ldots, d_R$) of the multiplet R an area law for the k-loop with charge Y_k, Eq. 30:

$$W_k(L)|_{\rm r} = \exp\left[-(1 - {\rm Re}\ D_R(Y_k)_{\rm r,r})\bar{\ell}\right]. \tag{48}$$

The k-dependence of the tension due to all members of the multiplet is then proportional to:

$$\sigma_k = [d_R - {\rm Re\,Tr}\ \{D_R(Y_k)_R\} = d_R - {\rm Re\,Tr}\ \{\exp(i\pi(Y_k)_R)\}]\, l_M n_M. \tag{49}$$

This result is invariant under a gauge rotation,

$$Y_k \to \Omega Y_k \Omega^\dagger \tag{50}$$

as Eq. 30 suggests. And it reduces to $2k(N-k)$ for the case where R is the adjoint. The reason is that $(Y_k)_{\rm adjoint}$ has either 0 or ± 1 on the diagonal as argued already in the previous section. Hence the formula counts the multiplicity of charged members of the adjoint multiplet.

For the spinor representation one finds from Eq. 49 the result quoted in Ref. [21]:

$$\sigma_k \sim [N - k\cos(((N-k)\pi/N)) - (N-k)\cos(k\pi/N))]. \tag{51}$$

Both adjoint and spinor multiplets are compared to the lattice data in the section on data analysis.

4.6 Corrections

There are two sources of corrections to the Casimir scaling formula. One is the diluteness, and the other are the effects of Bose-Einstein statistics.

- The diluteness $\delta = l_M^3 n_M = \sigma_1/m_M^2$ is small (~ 0.05, as discussed in section 2.2) but produces corrections. The use of classical Boltzmann statistics is allowed at large T, since the thermal de Broglie wave length $1/T$ is much smaller than the inter-particle distance $1/g^(T)T$.

- As we descend in temperature the diluteness stays constant, since we know from the results by Laine and Schroeder [38] that magnetic quantities are determined to a very good approximation through all of the plasma phase by their value at very large T in 3d Yang-Mills theory, and the running of the coupling due to hard radiative corrections. Below T_c σ_1 is virtually constant [30]. Unfortunately the behaviour of the magnetic mass is not known in the cold phase, but we know its value at $T = 0$ leading to a diluteness ~ 0.09(see section 2.2), which suggests that it is small at all temperatures.

- What changes as we go down in T is the ratio of thermal wave length to inter-particle distance. So Bose-Einstein statistics kicks in at temperatures on the order of $4T_c$, where $g^2(T) = \mathcal{O}(1)$. It seems natural that the transition is where Bose-Einstein condensation starts.

In principle the effects due to the small but non-zero diluteness can be computed. Comparison to lattice data [30] in the deconfined phase shows that they should be small, on the order of a few percent at most.

5 On strings in higher representations and $\frac{1}{N}$ corrections

We now leave the discussion of the adjoint-monopole-gas model and discuss the properties of k-strings from the point of view of the large-N expansion.

Standard arguments on large N SU(N) gauge theory [51, 52], based on the planarity of Feynman diagrams and the (assumed) confinement of color, imply that gauge invariant states have masses of order $N^0 + N^{-2}$, with a width of order N^{-2}. Also, no bound state of color singlet constituents survives the large N limit: the theory is expected to be a theory of free 'hadrons'.

It is interesting to consider, at large but finite number of colors, precisely those states whose wavefunction contains a significant component which is a direct product of color singlet pieces. Phenomenology provides a number of potential examples. A classic example would be the deuteron, a very loosely bound state lying only a few MeV under the nucleon-nucleon threshold. Another interesting though less firmly established case is the $f_0(980)$ meson, whose wavefunction has been discussed in terms of a mixture of a kaon-kaon molecule and a four-quark state ([55] and ref. therein). Again, the state is only a few MeV under the two-kaon threshold.

At a more theoretical level, there are examples in the pure SU(N) gauge theory in three and four dimensions. Consider the theory defined on a finite (but large: $L \gg 1/T_c$) hypertorus. In addition to glueballs, the spectrum contains 'torelon' states (whose mass we denote by $m_k(L)$) which transform non-trivially under the centre symmetry Z_N. The sectors of different $\mathcal{N}$-ality are protected by this global symmetry. Thus for $N \geq 4$, one may ask whether two fundamental torelons can form a bound state lying under the threshold $2m_{k=1}(L)$. That this is indeed the case was first numerically demonstrated from first principles in the work [25]. Further, at large L the states are string-like and one can ask what the ratios of their string tensions are (we may use the fundamental '$k = 1$' string tension as the reference). An alternative formulation of the problem would consider the strings to be open and attached to static sources in the appropriate representation [53].

For simplicity, we now focus on the $k = 2$ sector; for $N \geq 4$, the screening of the string is forbidden by the centre symmetry. In our view, the first question to settle in the context of the large-N expansion is, 'What is the $1/N$ power of the leading correction to the planar limit result $\sigma_2 = 2\sigma_1$?'. Since $m_2(L)$ lies under the threshold $2m_{k=1}(L)$ at all L [25], the question arises whether one should think of the $k = 2$ torelon as a weakly bound state of two $k = 1$ torelons, or if the colour structure gets completely rearranged into a single 'unfactorisable' color singlet piece. In the nucleon-nucleon system, the analogous question is whether the deuteron is primarily a bound state of two nucleons, or a 6-quark state. In the first case, considered in [39], the long-distance attractive force between the two $k = 1$ strings will be driven by the exchange of the lightest (0^{++}) glueball, while the short distance force is essentially given by two-gluon exchange. Both effects are indeed [39] suppressed by $1/N^2$ with respect to the free propagation of two $k = 1$ strings. Regarding the second configuration, the simplest classical string configuration is that of a single string winding twice around a cycle of the hypertorus. At large N , the energy of such a configuration is expected to approach threshold from below

at a $1/N^2$ rate.

At finite N and asymptotically large L however, we are in presence of two almost degenerate configurations lying near threshold. It is therefore imperative to consider the mixing effects between these two configurations. To keep the discussion as simple as possible, we may keep the transverse spatial dimensions $L_\perp$ finite, so as to separate two-torelon 'scattering states' from the weakly bound states we discuss by a finite, fixed gap. As N is increased, this transverse volume can be increased as well without affecting the validity of our treatment of the $k = 2$ sector as a 2-level system.

We suppose, following [34], that the Hamiltonian of the SU(N) gauge theory can be expanded in inverse powers of $1/N$:

$$H(L, N) = \sum_{k=0}^{\infty} \frac{H_k(L)}{N^k}. \tag{52}$$

The existence of the t'Hooft limit implies that $H_o(L)$ has the same eigenvalues as the Hamiltonian of the SU(∞) theory in the same spatial volume. We consider now the $k = 2$ flux tubes winding around a cycle of the torus as a quantum mechanical two-state system, as was done in [34] for the case of the scalar glueball – adjoint Polyakov loop system in intermediate volume. Consider on the one hand the state made of two $k = 1$ non-interacting closed fundamental strings, and on the other a single fundamental string with winding number 2; in this basis H_o reads $H_o = 2m_{k=1}\mathbf{I}_{2\times 2}$.

The 'perturbation' describes the deviations from the planar limit. On the diagonal, the corrections are $\mathcal{O}(1/N^2)$. Indeed, the attractive potential between two fundamental torelons is suppressed by the product of two 3-vertices each of which carries a $1/N$ factor. On the other hand, the amplitude of the transition from one of our basis states to the other only contains one such vertex, and therefore the off-diagonal element of our 2×2 hamiltonian is $\mathcal{O}(1/N)$. The perturbation hamiltonian in our basis reads:

$$\Delta H = \begin{pmatrix} -\bar{h}_1/N^2 & \bar{h}/N \\ \bar{h}/N & -\bar{h}_2/N^2 \end{pmatrix} \tag{53}$$

with $\bar{h}_1$, $\bar{h}_2$ and $\bar{h}$ of order N^0. It is clear that to leading order in $1/N$, the resulting energy eigenstates are now the symmetric and anti-symmetric linear combinations of our basis states. The associated energies are $E_A = 2m_{k=1} - \frac{\bar{h}}{N} + \mathcal{O}(1/N^2)$ and $E_S = 2m_{k=1} + \frac{\bar{h}}{N} + \mathcal{O}(1/N^2)$. We thus reached the perhaps surprising conclusion that the corrections to the mass of the lightest $k = 2$ string are of order $1/N$. There is one state below threshold and one above, situated symmetrically about the threshold energy, up to $O(1/N)$ corrections. We note that $\bar{h}$ (as well as the $\bar{h}_i$) is expected to grow proportionally to L at large L, since the breaking of the string can occur at any point along the string, so that the ratio in the torelon masses directly translates into the ratio of the string tensions.

A caveat particularly relevant to Monte-Carlo simulations is that in all the considerations above we have supposed the strings to be long enough to be able to identify the ratios of string tensions ratios with the ratio of torelon masses. Since the $1/L$ string correction [17] lowers the energy of the string, it induces a repulsive force between two fundamental torelons at finite

L [34]. Since the binding energy of the strings reduces at large N , L must be increased so that the condition

$$\sigma_1 L^2 \gg N \tag{54}$$

is satisfied to ensure that the ratio of torelon loops yields the correct N-dependence of the string tension ratios. If the large N limit is taken at finite L, the ratio of $k = 2$ to $k = 1$ torelon masses will approach 2 with $1/N^2$ corrections, because a mixing amplitude only affects the energy spectrum at leading order if the 'unperturbed' states are degenerate (to that order). And indeed, the two classical-string configurations we took as unperturbed states have different $1/L$ corrections: if γ_1 is the Lüscher coefficient of the fundamental string, the direct-product configuration of two $k = 1$ strings has a $2\gamma_1/L$ correction, while the fundamental string with winding number 2 admits a $\gamma_1/2L$ string correction. As all lattice simulations so far [25, 26, 29], ours are done in the regime $N < \sigma_1 L^2 < N^2$. The second inequality implies that the energy gap $(\bar{h}_1 - \bar{h}_2)/N^2$ is parametrically smaller than the string vibrational excitations.

Eq. 54 however also implies that the vibrational excitations of the strings are separated by $4\pi/L$ gaps which are parametrically much smaller than the mixing energy $\bar{h}/N$. We have thus neglected the matrix elements of the Hamiltonian H_1 between the two states that we focused on and the vibrationnally excited states, since we reduced the diagonalisation problem from the full Hilbert space to the space spanned by these two states. Although the neglected matrix elements can modify the splitting pattern around the threshold, the mixing between the string ground states will be enhanced relatively to the other mixings if the condition $\sigma_1 L^2 \ll N^2$ holds. In any case, the parametric size of these matrix elements is $\sigma L/N$ and so we must expect the corrections to the $k = 2$ string tension to be of that order.

In summary, the predictions of the two-state mixing model are:

1. the energy eigenstates are the anti-symmetric and the symmetric linear combinations of the direct-product configuration of two $k = 1$ strings and the fundamental string with winding number 2.

2. they are split symmetrically around the threshold energy $2m_1$ (up to $O(1/N)$ corrections).

3. the splitting energy itself is of order $1/N$.

5.1 Static potentials

If one considers open strings attached to static 'quarks', the argument takes a slightly different form. The relevant quantities here are the static potentials between colour sources in *irreducible* representations of SU(N).

The k=1 string binds a quark and a distant antiquark together. Similarly the k=2 configuration can be viewed as two (weakly interacting) strings each joining one of the quarks to one of the antiquarks. If we number the quarks by 1 and 2, and the antiquarks by $\bar{1}$ and $\bar{2}$, then there are two classical string configurations which are exactly degenerate: the configuration where 1 is attached by a string to $\bar{1}$ and 2 is attached to $\bar{2}$, and the other where 1 is attached to $\bar{2}$ and 2 to $\bar{1}$. However, the interaction between the strings can take one configuration into the other. Therefore a splitting occurs between the symmetric and anti-symmetric linear combinations, corresponding to the static potential splitting between the $k = 2$ symmetric and

anti-symmetric irreducible representations of SU(N). There is however general agreement that screening of the static sources through virtual gluons implies that the string tension obtained in either representation at large enough separations is the same; although it can be difficult to demonstrate this in Monte-Carlo simulations.

5.2 A caveat on the implications of factorisation at large N

The standard way to extract the static potential for fundamental charges, namely by measuring the expectation value of a rectangular Wilson loop of size $R \times T$, $T \gg R$, can be generalised to extract it for any representation [53]. In particular, the simplest way to obtain a representation of $\mathcal{N}$-ality $k = 2$ is to take the real part of the square of $W(R,T)$, the trace of the fundamental Wilson loop. At finite R, T, the factorisation property of gauge invariant operators (see for instance [56]) then implies that the expectation value of this operator is given by

$$\langle W(R,T)^2 \rangle = \langle W(R,T) \rangle^2 \ (1 + \mathcal{O}(1/N^2)). \quad \text{(factorisation)} \tag{55}$$

On the other hand, if we consider small separations R, asymptotic freedom implies that the short-distance potential in an irreducible representation $\mathcal{R}$ is given by $C_{\mathcal{R}} \alpha_s / R$. The symmetric $k = 2$ representation has $C_{\mathcal{R}} = C_S = 2(N+2)C_F/(N+1)$, while the $k = 2$ anti-symmetric has $C_A = 2(N-2)C_F/(N-1)$. In particular, for the fundamental representation, it is

$$W(R,T) = \exp\left(-\frac{\bar{\alpha} T}{2R}\right) \ + \ \mathcal{O}(1/N^2), \qquad R \ll \sigma^{-1/2}. \tag{56}$$

The operator $W^2(R,T)$ belongs to a representation that can be reduced into the symmetric and anti-symmetric. Therefore, if we take the $T \to \infty$ limit, the potential energy of the anti-symmetric representation dominates the expectation value of $W^2(R,T)$:

$$\lim_{T\to\infty} \langle W^2(R,T) \rangle \propto e^{-C_A \alpha_s C T/R} = \langle W(R,T) \rangle^2 \ e^{\frac{\bar{\alpha} T}{NR}} \ (1 + \mathcal{O}(1/N^2)), \quad R \ll \sigma^{-1/2}. \tag{57}$$

Thus tree-level perturbation theory contradicts the large-N counting rules concerning the leading corrections to factorisation. The origin of the paradox lies in the straightforward $T \to \infty$ limit necessary to filter out the ground state. If the contribution from the symmetric representation is kept, the large N limit of the small-R, large-T Wilson loop $\langle W^2(R,T) \rangle$ is given by

$$\lim_{T\to\infty} \langle W^2(R,T) \rangle \propto \langle W(R,T) \rangle^2 \ \cosh\left(\frac{\bar{\alpha} T}{NR}\right) \ (1 + \mathcal{O}(1/N^2)), \tag{58}$$

which, at fixed T, has $1/N^2$ corrections to the planar limit result.

What have we learnt? The large-N factorisation property does not necessarily imply that the lowest energy state of a 'meson' made of a static colour source in a certain representation and its anti-source has $\mathcal{O}(1/N^2)$ corrections, *because other representations of same $\mathcal{N}$-ality become degenerate with it in the $N \to \infty$ limit.* Since string tensions are extracted from the lowest energy at large R, the same caveat applies to them.

5.3 Strings in open and closed form

We finish with a remark on the relation between different representations of same $\mathcal{N}$-ality and excited states in the open and the closed string sectors. To that end it is useful to consider the correlator of Polyakov loops of length L $\langle P_{\mathcal{R}}(0)P_{\bar{\mathcal{R}}'}(\vec{x})\rangle$. This expectation value is interpreted (from the point of view of the transfer matrix along the dimension of size L) as the free energy of the system in the presence of two static charges in the given representations. When $\mathcal{R} = \mathcal{R}' = N$, the fundamental representation, the heavy-heavy bound state can a priori be in the adjoint or the singlet representation (in SU(3): $3 \otimes \bar{3} = 8 \oplus 1$). Now, it is believed that only bound states in the singlet representation have a finite free-energy in the confined phase. That means that if the heavy charges themselves are not in the singlet representation, virtual gluons will try and screen the chromoelectric field emanating from this coloured bound state until it is a singlet again. Since the gluons are in the adjoint representation, they can screen the configurations of the heavy-quark bound state that are in the adjoint representation, albeit at a certain energy cost. On the other hand they cannot screen a single heavy quark, and the latter therefore has an infinite free energy.

Suppose we want to determine the static potential for sources in all possible representations of SU(N) (not necessarily irreducible) of a given $\mathcal{N}$-ality k and up to a given size. Clearly it is sufficient to determine the Polyakov loop correlators between the irreducible representations obtained in the decomposition of the direct product representation of k quarks. The question then arises whether the cross-correlations (i.e. for $\mathcal{R} \neq \mathcal{R}'$) between Polyakov loops in these irreducible representations vanish or not. If they do, it implies that the energy eigenstates are in definite irreducible representations.

Consider the $k = 2$ case. The direct product of two fundamental representations decompose into a symmetric and an anti-symmetric representation: $N \otimes N = A \oplus S$. In the most familiar case of SU(3), the anti-symmetric representation is nothing but the $\bar{3}$ (anti-fundamental): $3 \otimes 3 = 6 + \bar{3}$. So we are asking whether $\langle P_S(0)P_{\bar{A}}(\vec{x})\rangle$ has to vanish. We have $6 \otimes 3 = 10 \oplus 8$, so that virtual gluons can screen the adjoint piece, thus ensuring that the free energy of this system is finite. So in general these cross-correlations do not vanish. It is easy to see (using Young tableaux) that in SU(N) the adjoint representation appears exactly once in the decomposition of $S \otimes \bar{A}$. However since gluons have to screen the heavy-heavy system, the $\langle P_S(0)P_{\bar{A}}(\vec{x})\rangle$ are $1/N^2$ suppressed at large N. Let us now see what this conclusion implies for the determination of the k-string tensions in the open and the closed string sectors.

In order to study the lightest open string, one may in principle choose to immerse any one static source of the relevant $\mathcal{N}$-ality in the system, since for large enough R the sources are expected to be screened down to the representation with the smallest string tension. Once the linear behaviour of $V(R)$ with the latter slope sets in, the differences between the static potentials in irreducible representations of same $\mathcal{N}$-ality are expected to become only weakly R-dependent (they correspond to 'gluelump' masses [54]). For long enough strings, the lowest excitations of any of these static 'mesons' correspond to the lowest excitations of that string, which come in gaps of order $1/R$. In short, there is at most one stable open string for a given $\mathcal{N}$-ality.

It is also possible to interpret the Polyakov loop correlator with a transfer matrix along the direction $\vec{x}$. One is then measuring the spectrum of states of the gauge theory which carry a

winding number with respect to a cycle of the hypertorus of length L. Of course, since the Polyakov loop correlator has a unique asymptotic area law, the coefficient in front of the area defines both the string tension in the open as in the closed string sector. Just as in the open string case, there cannot be more than one stable string per $\mathcal{N}$-ality because of the screening by gluons. A simple picture [25] is that virtual gluons screen the unstable string down to the stable one and propagate along it until they annihilate around the cycle of the torus.

For long enough torelons, the lowest closed-string excitations are again expected to be string-like, i.e. coming in $1/L$ gaps. There can be resonant states of the torelons (lying above the k-torelon threshold) whose energies grow linearly with L. It is then natural to associate them with meta-stable strings.

What we inferred about the cross-correlations between different irreducible representations above tells us that the energy eigenstates do *not* in general belong to irreducible representations of SU(N), although the mixing between them is suppressed (at least in the $k = 2$ case) by $1/N^2$.

6 Lattice simulations

We extract string tensions in the three-dimensional SU(8) gauge theory from the masses of 'torelons', gauge invariant states transforming non-trivially under the $Z(N)$ symmetry of the action; they wind around one spatial cycle of a the hypertorus. These masses are extracted from the exponential decay of correlation functions at 'large' Euclidean time. To enhance the signal-to-noise ratio, we use fuzzing techniques in the construction of our operators as described in [29]. The correlation functions are measured on gauge configurations generated by a Monte-Carlo program. We use the original Wilson action [59]. The configuration is updated by sequences of 'sweeps'. One sweep consists of updating all links by performing either a heat-bath (HB) [62] or an over-relaxation (OR) [63] step on $N(N-1)/2$ of its $SU(2)$ subgroups [61]. The ratio of HB:OR is 1:3, and we typically perform a sequence of 1 HB and 3 OR between measurements. We use a 2-level algorithm [32] as described in [33]. The latter reference also contains a detailed comparison of efficiency of the ordinary 1-level and 2-level algorithms. The number of measurements performed at fixed time-slices was 800 at $\beta = 115$, 200 at $\beta = 138$ and 40 at $\beta = 172.5$.

6.1 String corrections

Consider the Euclidean gauge theory on a $L \times L \times T$ hypertorus, with cycles of length L. The gauge-invariant states with winding number $k \neq 0$ around one spatial cycle of the hypertorus are called torelons. In the Hamiltonian language they are created by spatial Polyakov-loop operators with $\mathcal{N}$-ality k; a description of the operators used can be found in appendix C. If the dynamics of a torelon state of length $L\sqrt{\sigma} \gg 1$ is described by an effective string action, then the expression for its mass as a function of its length reads

$$m(L) = \sigma L \left[1 - \frac{\gamma}{\sigma L^2} + \mathcal{O}\left(\frac{1}{\sigma L^2} \right)^2 \right], \tag{59}$$

where γ is a numerical coefficient of order one which only depends on the universality class of the string [17]. Recent accurate numerical results [57, 25] show that the flux-tube in the fundamental representation belongs to the bosonic string class. In the case of a torelon this implies that

$$\gamma = \gamma_b \equiv \frac{(D-2)\pi}{6}. \tag{60}$$

In general, if Eq. 59 holds, the ratio of the lightest k-torelon mass to the $k = 1$ torelon mass is given by

$$\frac{m_k}{m_1}(L) = \frac{\sigma_k}{\sigma_1} + \frac{\alpha_k}{\sigma_1 L^2} + \mathcal{O}\left(\frac{1}{\sigma_1 L^2}\right)^2 , \qquad \alpha_k = \frac{\gamma_1 \sigma_k}{\sigma_1} - \gamma_k \tag{61}$$

The sign of α_k is of interest. If the k-string is a weakly bound state of k fundamental strings, then one would expect $\gamma_k = k\gamma_1$ and therefore $\alpha_k = -(k - \frac{\sigma_k}{\sigma_1})\gamma_1 < 0$. If one the other hand the fluctuations of the k fundamental strings are 'in phase', then the number of degrees of freedom on the worldsheet of the k-string is the same as for the fundamental string, hence $\gamma_k = \gamma_1$ and $\alpha_k = (\frac{\sigma_k}{\sigma_1} - 1)\gamma_1 > 0$.

At each lattice spacing, we measured the masses of the torelon states of at least three different lengths. In practice, we use two asymmetric lattices of the type $L_1 \times L_2 \times L_t$ and $L_2 \times L_3 \times L_t$. In this way, we obtain three different lengths of the torelon, and we can also check for any dependence on the transverse size of the lattice by comparing the mass obtained for the torelon of length L_2 on the two lattices. The L_i range from 1.4fm to 3fm, if we set the scale by $\sqrt{\sigma_1} = 440$MeV. This is longer than what has been normally measured so far, and is made possible by the use of the two-level algorithm. We use Eq. 59 to obtain the fundamental string tension by fitting $m(L)/L$ with a linear function in $1/L^2$. The intercept yields the string tension; the slope gives the Lüscher coefficient. Whether the functional form (59) successfully describes the leading deviation from constant linear mass density is controlled by the χ^2 of the fit.

Systematic errors play an important role in comparing the numerical data to model predictions. In an attempt to get them under control we propose two separate ways to extract the ratios of string tensions (we refer to the first method as the 'unconstrained' one, and the second as the 'constrained' one). In practice, having learnt from the pros and contras of both data analyses, we present our final, 'educated' analysis in section 6.2.4.

1. Firstly the ratios of torelon masses $m_k(L)/m_1(L)$ are fitted according to Eq. 61 with a linear function in $1/L^2$, and the intercept gives us the ratio $\frac{\sigma_k}{\sigma_1}$. In this way, we need make no assumption about the values of the coefficients γ corresponding to the different representations; in particular, the different strings could have different coefficients γ_k. Finally, these string ratios are extrapolated to the continuum, $a \to 0$, in a standard way.

2. The second analysis will *assume* that all k-strings belong to the bosonic class. Consequently, we can extract the string tension ratio from Eq. 61 using the estimate $\alpha_k \simeq \frac{m_k \gamma_1}{m_1} - \gamma_k$ with $\gamma_k = \gamma_1 = \gamma_b$ at every L. The estimates of the ratios obtained at different L are then simply averaged, as long as they are compatible with eachother, to produce the estimates of

the string-tension ratios. If the χ^2 of the average is large, we drop the smallest L until an acceptable χ^2 is reached. The continuum limit is then taken.

The multi-level algorithm allows us to apply the variational method [60] on the correlation matrices at $t \geq 2a$ of Euclidean time separation, an improvement over the traditional where the method is usually unstable unless $t = 0$, although the method really finds its justification when applied at large t.

Having said that, we note that this work constitutes the first attempt to extract the $k = 4$ string tension from Monte-Carlo simulations, and should be regarded as exploratory in that sector. Indeed we found that the variational method [60] generally became unstable if all five operators listed in appendix C were fed in the generalised eigenvalue problem. As a consequence only three or four of the five types of measured operators (at the 'best' level of smearing-blocking) were finally employed. This and the fact that we only have a short range in Euclidean time to identify the mass plateau, due to the rapid fall-off of the signal, means that the $k = 4$ string tension has a significant systematic error attached to it. For the lower k states, these problems are less accute and we are much more confident about their mass estimates.

6.2 Data analysis

We give the masses of the lightest spatial torelons of each $\mathcal{N}$-ality in Tab. 1; Tab. 4 gives estimates of the first-excited torelon mass in the $k = 2$ sector, that will be discussed below. Within the range considered ($L \simeq 1.9$fm, $0.8L \leq L_\perp \leq 1.2L$), we certainly find no dependence of the $k = 1$ torelon masses on the transverse size. There is also no statistically significant variation of the lightest higher-k torelon masses. Transverse size corrections are expected to be suppressed by a power of $1/L$ varying continuously with $L_\perp$, but greater than 3 [58].

We show on Fig. 6 the local effective mass of the correlators in the $k = 1$ and $k = 2$ representations. We emphasize that the variational method, which yields (quasi-)orthogonal states, automatically picks out the symmetric and anti-symmetric linear combinations (within very small fluctuations on the coefficients). We shall come back to this point in the discussion below, section 6.3.

6.2.1 Setting the scale

Although one could choose the (dimensionful) coupling to set the scale, we prefer to use $\sqrt{\sigma_1}$ for this purpose. We extract the fundamental string tension in lattice units at each of our three lattice spacings by linearly extrapolating the torelon mass per unit length, m_T/g^4L as a function of $1/(g^4L^2)$, to infinite L. This is illustrated by Fig. 4 in the case $\beta \equiv \frac{2N}{ag^2} = 138$. The resulting string tensions are given in Tab. 2. We are able to extract the coefficient of the $1/R$ string correction with moderate accuracy; it is also given in Tab. 2. The coefficients we obtain are within 1.3 standard deviations of the bosonic string value.

Similarly, we can extract the $k = 2$ string tension and its string correction coefficient γ_2 (Fig. 4, bottom plot). It is clear however that the accuracy of the data does not allow us to estimate γ_2.

6.2.2 Unconstrained extrapolations

In this analysis, for each lattice spacing we extrapolate the ratios of k-torelon masses to $L = \infty$, assuming $1/(g^2L)^2$ corrections. In most cases, we have three torelon lengths to extrapolate. For the intermediate length, where we have two statistically independent and compatible values obtained at different transverse sizes of the spatial lattice, the average (weighted by the inverse square of the statistical error) of the two values was taken, whilst keeping the smaller of the two errors. In the ratio of the k-torelon to the $k = 1$ torelon mass obtained in the same simulation, we checked in several cases that the error bars obtained by assuming statistical independence do not differ by more than 10% from the jacknife values of the error bars; the former are then used in the following.

We note that the results of these extrapolations done at different lattice spacings are in fact consistent within error bars (see Tab. 2); it appears that finite lattice spacing effects are much smaller than the finite string-length effects in our data set. The χ^2 of each of these fits are good (smaller than 1), except for the extrapolation of the σ_2/σ_1 at $\beta = 172.5$, where $\chi^2 = 3.0$. Since the $L = \infty$ extrapolated value is entirely consistent with that obtained at the other values of β, we attribute this to a statistical fluctuation and, perhaps, a slight underestimation of the error bars (due to the neglect of the sort of systematic errors mentioned at the end of section 6.1).

Now extrapolating these string tension ratios to the continuum (assuming $\mathcal{O}(\sigma_1 a^2)$ discretisation errors), we obtain $\sigma_2/\sigma_1 = 1.701(77)$, $\sigma_3/\sigma_1 = 2.31(16)$ and $\sigma_4/\sigma_1 = 1.96(23)$. The χ^2 of these fits are smaller than 1. The final error bars have blown up due to a somewhat small level-arm in the continuum extrapolation.

6.2.3 Constrained analysis

In this independent analysis, we assume the validity of Eq. 59 with γ given by the bosonic string value Eq. 60 to extract the string tensions at finite L (neglecting the $\mathcal{O}(1/L^4)$ terms); see the string tension ratios in Tab. 3, where again statistical errors have been added in quadrature. In most cases, these ratios are consistent with being independent of L for $L \geq 1.4$fm. The exceptions concern the $k = 2$ string at the two smaller lattice spacings (due to the accuracy of the data), where we drop the smallest L in our average. We note that, compared to the values of the unconstrained analysis (Tab. 2), the ratios are systematically larger. The ratios for the k-strings in the continuum limit now are: $\sigma_2/\sigma_1 = 1.776(33)$, $\sigma_3/\sigma_1 = 2.210(50)$ and $\sigma_4/\sigma_1 = 2.282(63)$. The χ^2 of the fits are again smaller than 1.

6.2.4 Final 'educated' analysis

We consider the preceding analysis to be somewhat unsatifactory, because it assumes a specific correction to the k-string energies which we are not presently able to confirm directly (see Fig. 4), and yet (in the $k = 2$ case) is of the same order of magnitude as the difference between two theoretical expectations we are to compare our data to. Moreover we saw that the string tension ratios obtained in this way are systematically higher than if we do not make any assumptions about the Lüscher coefficients, although the trend is at the one-standard-deviation level.

The first analysis is well-principled but suffers from the succession of extrapolations to $L = \infty$ and $a = 0$, most of which are based on three data points only and are therefore rather unstable. Considering the large-L extrapolation (Fig. 5, in particular the $k = 2$ plot), we see that while the coarsest lattice spacing data still shows a difference with respect to the other two data sets, the latter two essentially fall on a single curve. Therefore we drop the $\beta = 115$ data and combine the data at $\beta = 138$ and $\beta = 172.5$ to do a single extrapolation to $L = \infty$. The result is:

lattice (final)	adj.monop.	fund.monop.	trigonometric	
$\sigma_2/\sigma_1 = 1.707(28)$	1.714	2.105	1.848	
$\sigma_3/\sigma_1 = 2.182(55)$	2.143	2.958	2.414	(62)
$\sigma_4/\sigma_1 = 2.203(82)$	2.286	3.256	2.613.	

(the χ^2 are respectively 3.5/5, 2.35/4 and 2.6/4). One ought to associate a systematic error with this final result which is of the same order as the statistical error, since evidence for the absence of scaling violations was given only at that level of accuracy. We also note that the slope, which corresponds to the quantity α_k defined in section 5, is clearly positive, clearly demonstrating that the central charge of a k-string is not k times that of the fundamental string.

It is hoped that presenting different analysis strategies has given the reader a sense of the challenge presented by these calculations to reduce the systematic errors on the final string tension ratios. Comparing our data to the theoretical predictions of various models (Eq. 62) we find that our data is consistent with the Casimir scaling predicted by the adjoint monopole model, and rules out the sine formula by at least 3 standard deviations at all k (even if we conservatively assign to the data a systematic error equal to the statistical one). These conclusions agree with earlier results obtained for SU(4) and SU(6) [25], although the accuracy was high enough for $N = 4$ to see a (non unexpected) small deviation from Casimir scaling.

6.3 Excited $k = 2$ strings

Fig. 6 shows the local effective masses, defined as $m_{\rm eff}(t + \frac{a}{2}) \equiv \log\left(\frac{C(t)}{C(t+a)}\right)$, of several of our operators; a plateau is the signature that an energy eigenstate is saturating the correlator. We show the local effective mass for our best $k = 1$ operator. The latter has been determined by a variational method [60] allowing to minimise the contributions from excited states to the correlator. Although several levels of fuzzing were included in the variational basis, the output wave function turned out to be dominated by a single level of fuzzing. We note that its plateau extends out to $t \simeq \sigma^{-1/2}$, giving as confidence in our mass extraction. In the $k = 2$ sector, we show local effective masses corresponding to the same level of fuzzing that was optimal for the $k = 1$ sector (the inclusion of other fuzzing levels leads to imperceptible changes in the mass plateaux). After the basis operators had been normalised in such a way that $\langle O_i(0) O_i^*(t = 0)\rangle = 1$ $(i = 1, 2)$, the variational procedure selected (within $O(1\%)$ error bars) the anti-symmetric and the symmetric linear combinations of the operators $O_1 \equiv \mathrm{Tr}\,\{P^2\}$ and $O_2 \equiv (\mathrm{Tr}\,P)^2$ for respectively the lightest state and the first excited state. Correspondingly these operators show quite convincing mass plateaux. By comparison, the individual operators

have a less good overlap onto the lightest state, although the signal extends far enough in Euclidean time to see that this overlap is not strongly suppressed: their local-effective-masses end up being consistent with the plateau of the anti-symmetric combination. Remarkably their whole correlators seem to agree at all t.

Thus the theoretical expectation that the energy eigenstates belong to irreducible representations of SU(N) up to $O(1/N^2)$ admixtures, which was motivated both in the two-state mixing model and by more general arguments about the N-dependence of screening (resp. sections 5 and 5.3), is indeed well verified.

Another prediction of the two-state mixing model presented in section 5 is that the lightest and the first-excited states should be split symmetrically around the threshold energy of $2m_{k=1}$ (to leading order in $1/N$). This is tested quantitatively in Tab. 4, which directly compares $2m_{k=1}$ to $\frac{1}{2}(m_{k=2} + m^*_{k=2})$. The latter two quantities are remarkably close for all string lengths and lattice spacings, and in many cases they are compatible within the quite small error bars[4].

As we discuss next, the numerical evidence obtained so far favours a binding energy of k-strings of order $1/N$. The three predictions that follow straightforwardly from the two-state mixing model presented in section 5 have thus been verified quantitatively.

6.4 N-dependence of the binding energy of k-strings

On Fig. 7 (top) we show the relative binding energy of k-strings per unit length, $k\sigma_1 - \sigma_k$, in units of σ_1 and rescaled by a factor N. We do so by compiling our SU(8) lattice data with the SU(4) and SU(6) data from [25]. The predictions of Casimir scaling and of the Sine formula are also plotted. The figure certainly suggests that the $k = 2$ binding energy scales as $1/N$, with a coefficient of order one. By contrast, to account for the measured $N = 8$, $k = 2$ binding energy in a $1/N^2$ expansion, the first coefficient would have to be about 20. We further note that the numerical agreement between the Casimir scaling prediction and the lattice data is quite remarkable. If anything, it lies somewhat above the lattice data, indicating that the k-strings are slightly less tightly bound that the Casimir formula suggests.

On the bottom plot, we show the $k = N/2$ string tension, rescaled by a factor $2/N$, as a function of $1/N$. The data is plausibly heading towards a finite value at $N = \infty$. Here too, Casimir scaling offers a good description of the data. Note that it predicts that the binding energy of the $k = N/2$ string is half of the energy of k non-interacting fundamental strings. The case $k = N/2$ is special in that the relevant operators (listed in appendix C) and their complex conjugate can mix through the appearance of the baryonic vertex on the string. Pictorially it swaps the oriented string from on orientation to the other. Naturally the eigenstates of the Hamiltonian are also eigenstates of the charge conjugation operator, i.e. the real and imaginary parts of the operators, which are respectively $C = +$ and $C = -$. However the existence of a non-vanishing transition probability between the strings of definite orientations means that there is a splitting between the $C = +$ and the $C = -$ states of $\mathcal{N}$-ality $N/2$ (for $k < N/2$, the center symmetry forces the degeneracy of these two sets of states). In a two-state Hamiltonian formalism, the Casimir formula thus suggests that the Hamiltonian matrix element (per unit

[4] As a technical aside, we note that it is essential here to use the correlations between the local effective mass of the lightest and the first-excited $k = 2$ states, as they seem to be strongly anti-correlated.

length of the string) associated with the baryon-vertex is $\frac{N}{2}\sigma$.

It should be noted that the cost of computing the binding energy for a given k naively increases as N^5 (N^3 for the cost of multiplying SU(N) together in the Monte-Carlo simulation and a $\propto N^2$ increase of the statistics to compensate for the $1/N$ size of the binding energy). And this does not even take into account the condition $\sigma_1 L^2 \gg N$ formulated in section 5. Therefore it could be useful to also compute the string tension ratios for SU(5) and SU(7) before moving to even larger groups.

7 Conclusion

The picture of hot multi-color QCD considered in this paper relies on the separation of the hard, soft and ultra-soft scales by means of a well-known sequence of two effective theories. The second of these, which describes the magnetic properties of the quark-gluon plasma at energies of order $g^2(T)T$, is the 3D SU(N) gauge theory obtained by dimensionally reducing the original theory.

In the case of the spatial t'Hooft k-loop, which records the fluctuations of the electric flux of $\mathcal{N}$-ality k going through it, perturbation theory is directly applicable and becomes ever more accurate at higher temperatures. On the other hand, a simple physical picture emerges if the electric-flux fluctuations are attributed to gluons passing randomly through it. By assuming these quasi-particles to be dilute and non-interacting, one easily derives an expression whose parametric dependence on the temperature and the $\mathcal{N}$-ality of the loop match the perturbative result.

The adjoint monopole gas model discussed in this paper assumes a similar picture to hold for the spatial Wilson k-loops: the magnetic-flux is attributed to non-Abelian monopoles in the 3D SU(N) theory. The assumption that these monopoles are in the adjoint representation directly leads to the prediction of Casimir scaling for the ratios of the associated k-string tensions. The k-dependence is indeed given by the multiplicity of charged monopoles with respect to the charge Y_k of the loop, while the sensitivity to other details of the model is reduced in these ratios. Perturbation theory is not applicable in this sector, but non-perturbative lattice Monte-Carlo calculations of the k-string tension ratios, although numerically challenging, are in principle straightforward.

Previous simulations [25] for $N = 4,\ 6$, as well as the $N = 8$ data presented in this paper confirm the Casimir scaling property of k-string tension at the few percent level. Care must be taken in these calculations that the strings are long enough, $\sigma L^2 \gg N$, for the quantum corrections to the string energy to be subleading with respect to the weak binding energy of the k fundamental strings. The energy of the string is then large and a multi-level algorithm [32] proved useful in this situation to reduce the variance on the correlator from which this energy is extracted. While the Casimir scaling prediction lies slightly above the 3-loop expression for the t'Hooft loop, it is slightly lower than the lattice results for spatial Wilson loops: the (small) corrections to Casimir scaling in the magnetic sector seem to have the opposite sign with respect to the electric sector.

The fundamental assumptions of the model can be further tested. The behaviour of k-loops, as we argued, is the simplest observable to consider. It can be measured for other gauge

groups, as long as the center is $Z(N)$, $N \geq 4$; indeed the adjoint monopoles may be formed in *any* non-Abelian gauge theory. The classical groups have as candidates, apart from the SU(N) groups, the Spin($4p+2$) groups with center group $Z(4)$. One may also introduce an adjoint Higgs field which acquires a VEV. Depending on the symmetry breaking pattern, some monopoles will become heavy, and the k-ratios will change in a predictable way [47].

We also discussed the behaviour of the 't Hooft loops for different $\mathcal{N}$-alities at finite temperature. Here the same Casimir scaling is observed in the lattice data [27, 28] as predicted by perturbation theory for high T (and by the quasi-particle picture of gluons). Surprisingly, the scaling continues to hold down to practically T_c. And the same is true for the magnetic k-loops [38, 30]: Casimir scaling stays valid down to $\sim T_c$.

In conclusion: all available data on electric and magnetic k-loops for $N \geq 4$ are consistent with a screened electric and magnetic quasi-particle model throughout all of the plasma phase. Whether the same is true for QCD ($N = 3$) remains to be tested.

Acknowledgements

We acknowledge discussions with Pierre van Baal, Sander Bais, Nick Dorey, Philippe de Forcrand, Pierre Giovannangeli, Prem Kumar, Mikko Laine, Nick Manton, Hugh Osborne, Owe Philipsen, Martin Schvellinger, Jan Smit, and Mike Teper. Finally to Tony Kennedy, Tony Gonzalez-Arroyo and participants of the lattice Meeting (March 2005 at KITP Santa Barbara).

The lattice simulations were performed on the PC cluster of the Rudolf Peierls Centre for Theoretical Physics at Oxford University in the year 2004. The machine was partly funded by EPSRC and PPARC grants.

References

[1] G. 't Hooft, in High Energy Physics, ed. A. Zichichi (Editrice Compositori Bologna, 1976); S. Mandelstam, Phys. Rep. 23C (1976), 245

[2] G.'t Hooft, Nucl.Phys.B79:276, 1974; A. M. Polyakov (Landau Inst.), JETP Lett.20:194, 1974, Pisma Zh.Eksp.Teor.Fiz.20:430, 1974.

[3] P. Goddard, J. Nuyts, D. A. Olive, Nucl. Phys.B125 (1977), F. Englert, P. Windey, Phys. Rev.D 14(1977), 2728.

[4] F.A. Bais, J.R. Primack, Nucl.Phys.B123:253,1977; F. A. Bais, Phys.Rev.D18:1206,1978. E. J. Weinberg, Nucl. Phys. B167 (1980), 500.

[5] P. Goddard, D. I. Olive, Nucl.Phys.B191, 511 (1981); P. Goddard, D. I. Olive, Nucl.Phys.B191, 528 (1981).

[6] F. A. Bais, B. J. Schroers, Nucl. Phys. B512, 250 (1998), hep-th/9708004; Nucl.Phys.B535:197-218,1998; hep-th/9805163.

[7] R.A. Brandt, F. Neri, Nucl. Phys. B 161 (1979), 253. S. Coleman, Proceedings of the 1981 Erice School, Ed. A. Zichichi, Plenum (New York), (1982).

[8] A. Abouelsaoud, Nucl.Phys.B 226 (1983), 309; P. N. Nelson, A. Manohar, Phys. Rev. Lett.50 (1983), 943; A. Balachandran et al., Phys. Rev. Lett. 50 (1983) 1553; P. N. Nelson, S.R. Coleman, Nucl.Phys.B237:1,1984; N. Dorey, C. Fraser, T. J. Hollowood, M. A.C. Kneipp; hep-th/9512116.

[9] A. Hanany, D. Tong, JHEP 0307 (2003) 037, hep-th/0306150; A. Gorsky, M. Shifman, A. Yung, Phys.Rev.D71:045010,2005, hep-th/0412082;

[10] P. Irwin, Phys.Rev.D56:5200-5208,1997, hep-th/9704153; K-M. Lee, E. J. Weinberg, P. Yi, Phys.Rev.D54:6351,1996,hep-th/9605229;

[11] J. E. Humphries, Introduction to Lie Algebras and Representation Theory, Springer, New York.

[12] For a discussion of thermal screening of pointlike monopoles, see C. Manuel, Ann. Phys.263 (1998), 238.

[13] A.D. Linde, Phys. Lett.B 96,289 (1980).

[14] A. M. Polyakov, Nucl.Phys.B120, (1977), 429.

[15] S. Jaimungal, G.W. Semenoff and K. Zarembo, hep-th/9811238. Unpublished work by D. Diakonov and M. Chernodub (1999), private communication by D. Diakonov.

[16] G. 't Hooft, Nucl.Phys.B190, 455, 1981.

[17] M. Luescher, K. Symanzik and P. Weisz, Nucl. Phys. B **173** (1980) 365; M. Luescher, Nucl. Phys. B **180** (1981) 317.

[18] T. Bhattacharya, A. Gocksch, C.P. Korthals Altes, R. D. Pisarski, Nucl.Phys.B 383, (1992),497; Phys.Rev.Lett.66,998 (1991); C.P. Korthals Altes, Nucl.Phys.B420 (1994), 637.

[19] P. Giovannangeli, C. P. Korthals Altes, Nucl. Phys.B608, 203, (2001).

[20] P. Giovannangeli, C. P. Korthals Altes, to appear in Nucl. Phys.B.; hep-ph/0412322, hep-ph/0212298.

[21] C. P. Korthals Altes, invited talk at "Continuous Advances in QCD", Minnesota, 13-16 May 2004, to appear in the Proceedings; hep-ph/0408301.

[22] F. Gliozzi, hep-th/0504105.

[23] T. C. Kraan, P. van Baal, Phys.Lett.B435:389-395,1998; hep-th/9806034.

[24] M. Teper, Phys. Rev. D59 (1999) 014512; hep-lat/9812344.

[25] B. Lucini and M. Teper, Phys. Rev. **D64**, 105019 (2001), hep-lat/0107007.

[26] L. Del Debbio, H. Panagopoulos, P. Rossi and E. Vicari, JHEP **0201** (2002) 009 [arXiv:hep-th/0111090].

[27] P. de Forcrand, B. Lucini, M. Vettorazzo; hep-lat/0409148

[28] F. Bursa, M. Teper; hep-lat/0505025.

[29] B. Lucini, M. Teper and U. Wenger, JHEP 0406:012,2004; hep-lat/0404008.

[30] B. Lucini, M. Teper, U. Wenger, JHEP 0502 (2005) 033; hep-lat/0502003.

[31] P. de Forcrand, C.P. Korthals Altes, O. Philipsen, to appear.

[32] H. B. Meyer, JHEP **0301** (2003) 048, hep-lat/0209145.

[33] H. B. Meyer, JHEP **0401** (2004) 030, hep-lat/0312034.

[34] H. B. Meyer, JHEP 0503:064,2005; hep-lat/0412021.

[35] T. Applequist, R.D. Pisarski, Phys.Rev.D23,2305,(1981); P. Ginsparg, Nucl.Phys.B170,388, (1980). E. Braaten and A. Nieto, Phys. Rev. D 51 (1995) 6990 ;hep-ph/9501375. K. Farakos, K. Kajantie, K. Rummukainen, M. E. Shaposhnikov, Nucl.Phys.B425:67, 1994; hep-ph/9404201.

[36] S. Z. Huang, M. Lissia, Nucl.Phys.B438,54,1995; hep-ph/9411293.

[37] K. Kajantie, M. Laine, K. Rummukainen, M. Shaposhnikov, Nucl.Phys.B503:357; hep-ph/9704416.

[38] M. Laine, Y. Schroeder, hep-ph/0503061.

[39] A. Armoni and M. Shifman, Nucl. Phys. B **664** (2003) 233, hep-th/0304127; A. Armoni and M. Shifman, Nucl. Phys.B 671.67 (2003), hep-th/0307020.

[40] A. Hanany, M.J. Strassler, A. Zaffaroni, Nucl.Phys B513, 87 (1998), hep-th/9707244; C.P. Herzog, I. R. Klebanov, Phys. Lett.B526, 388 (2002), hep-th/0111078.

[41] C. P. Korthals Altes, A. Kovner, Phys. Rev D62, 096008, 2000; hep-ph/0004052.

[42] C. P. Herzog, Phys. Rev.D 66, 065009; hep-th/0205064.

[43] D. J. Gross, W. Taylor, Nucl.Phys.B403:395,1993; hep-th/9303046 .

[44] S. Bronoff, C. P. Korthals Altes, Phys.Lett.B448:85, 1999; hep-ph/9811243.

[45] K. Kajantie, M. Laine, A. Rajantie, K. Rummukainen, M. Tsypin, JHEP 9811:011,1998; hep-lat/9811004.

[46] A. Rajantie, Nucl. Phys.B 501, 521; hep-ph/9702255.

[47] C.P. Korthals altes, A. Rajantie, in preparation.

[48] P. Giovannangeli, Phys.Lett.B585:144, 2004; hep-ph/0312307; hep-ph/0506318.

[49] D. Diakonov, V.Yu. Petrov, Phys.Lett.B224:131, 1989; D. Diakonov and V. Petrov, J. Exp. Theor. Phys. **92** (2001) 905 [arXiv:hep-th/0008035].

[50] F. V. Gubarev, Phys. Rev. D **69** (2004) 114502 [arXiv:hep-lat/0309023]. B. Broda, arXiv:math-ph/0012035. D. Diakonov and V. Petrov, J. Exp. Theor. Phys. **92** (2001) 905 [arXiv:hep-th/0008035].

[51] G. 't Hooft, Nucl. Phys. B **72** (1974) 461.

[52] E. Witten, Nucl. Phys. **B160**, 57 (1979).

[53] S. Deldar, Phys. Rev. **D62**, 034509 (2000), hep-lat/9911008; G. S. Bali, Phys. Rev. **D62**, 114503 (2000), hep-lat/0006022.

[54] N. A. Campbell, I. H. Jorysz and C. Michael, Phys. Lett. B **167** (1986) 91.

[55] F. E. Close and N. A. Tornqvist, J. Phys. G **28** (2002) R249 [arXiv:hep-ph/0204205].

[56] S. R. Das, Rev. Mod. Phys. **59** (1987) 235.

[57] M. Luescher and P. Weisz, JHEP **07**, 049 (2002), hep-lat/0207003.

[58] H. B. Meyer, arXiv:hep-th/0506034.

[59] K. G. Wilson, Phys. Rev. D **10** (1974) 2445.

[60] M. Luscher and U. Wolff, Nucl. Phys. **B339**, 222 (1990).

[61] N. Cabibbo, E. Marinari, Phys. Lett. B119(1982) 387

[62] K. Fabricius, O. Haan, Phys. Lett B143 (1984) 459;
A.D. Kennedy, B.J. Pendleton, Phys. Lett., 156B (1985) 393

[63] S.L. Adler, Phys. Rev. D 23 (1981) 2901

Appendix A

In this appendix we briefly indicate the group theory needed to get from a given Young tableau (defining the irreducible representation R) the corresponding highest weight and the value of the quadratic Casimir. In what follows we suppose a representation to be irreducible without mentioning so. We choose the Y_k as follows:

$$Y_k = \frac{1}{N}\,\mathrm{diag}(\underbrace{k, k, \ldots, k}_{N-k \text{ times}}, \underbrace{k-N, k-N, \ldots, k-N}_{k \text{ times}}). \tag{63}$$

Let the Young tableau have n_1 boxes in the first row, n_2 in the second row, etc... Then one can define the non-negative numbers $w_l = n_l - n_{l+1}$. Now the highest weight matrix for the Young tableau is defined through the Y_k matrices:

$$H_R = \sum_{l=1}^{N-1} w_l Y_l. \tag{64}$$

For example, for the totally antisymmetric tableau of k boxes in one column we have $H_R = Y_k$. For the totally symmetric tableau with all k boxes in one row $H_R = kL_1$. Note that the stability group of Y_k (the subgroup of SU(N) matrices commuting with Y_k) is SU(k)$\times$SU($N-k$)$\times$U(1). So the totally antisymmetric representation with k squares has a highest weight with this stability group. All other representations with k squares have different stability groups.

We define one more diagonal $N \times N$ matrix by:

$$2Y \equiv 2\sum_{l=1}^{N-1} Y_l = \mathrm{diag}(N-1, N-3, ..., -N+1). \tag{65}$$

The quadratic Casimir operator $C_2(N, k, \{w_l\}) \equiv C_2(R)$ is defined by summing the square of all generators T_a in the representation R. The result is $\sum T_a^2 = C_2(R) 1_R$, where 1_R is the unit matrix in R and $C_2(R)$ is a c-number (normalization is $[T_a, T_b] = i f_{abc} T_c, f_{abc} f_{bcd} = N\delta_{ad}$). Then the quadratic Casimir equals:

$$C_2(R) = \frac{1}{2}(\mathrm{Tr}\,\{H_R^2\} + 2\mathrm{Tr}\,\{Y H_R\}). \tag{66}$$

The quadratic Casimir for the fundamental representation is $C_F = \frac{(N^2-1)}{2N}$. The Casimir for the antisymmetric representation is then

$$C_2(R = AS) = C_F \frac{k(N-k)}{(N-1)}, \tag{67}$$

and for the symmetric representation it is:

$$C_2(R = SS) = C_F \frac{k(N+k)}{(N+1)}. \tag{68}$$

To derive these relations one needs the inner product of two Y matrices:

$$\mathrm{Tr}\,\{Y_k Y_l\} = \frac{1}{N}(\min(k,l)N - kl). \tag{69}$$

One can show that for fixed $k \leq N$ the antisymmetric Casimir is the minimal one.

Finally we give the relation between the Y_k matrices and the Chevalley basis $H_{k,k+1} = \mathrm{diag}(0,0,0,....1,-1,0,...0)$, $Y_{N,N+1} \equiv Y_{N,1}$. We introduce the matrices y_k, with $y_1 \equiv NY_1$. y_2 follows from y_1 by a cyclic permutation of the diagonal elements: the first becomes the second and so forth. y_3 follows from y_2 the same way. We keep doing this until we have reached y_N, $y_{N+1} = y_1$. The sum of all the y_k vanishes. The Y_k are related to the y_k by:

$$NY_k = \sum_{l=1}^{k} y_l. \tag{70}$$

Then:

$$\begin{aligned}
\frac{1}{2}y_1 &= (N-1)H_{12} + (N-2)H_{23} + (N-3)H_{34} + ... + 1.H_{N-1N} + 0.H_{N1} \\
\frac{1}{2}y_2 &= 0.H_{12} \quad + (N-1)H_{23} + (N-2)H_{34} + ... + 2.HN-1N + 1.H_{N1} \\
\frac{1}{2}y_3 &= 1.H_{12} \qquad\qquad + 0.H_{23} + (N-1)H_{34} + ... + 3.HN-1N + 2.H_{N1}
\end{aligned}$$

The general term is:

$$\frac{1}{2}y_k = (k-2)H_{12} + (k-3)H_{23} + ... + 0.H_{kk-1} + (N-1)H_{kk} + ... + kH_{N-1N} + (k-1)H_{N1}. \quad (71)$$

Note the diagonal translation invariance of the coefficient matrix M relating the N y_k to the N $H_{l,l+1}$.

Evaluate the first diagonal element of the r.h.s. in Eq. 70, using the matrix M above. It equals, because of the relative sign in the non-zero elements of H_{12} and H_{N1}, the difference of the first column and the last column of M, up and including the first k rows of M. Because of the translation invariance only the difference $M_{11} - M_{kN} = N - k$ survives. The second diagonal element equals $M_{k1} - M_{12} = N - k$. This goes on till we reach the coefficient $M_{kk-1} = 0$. Then there is a jump to $M_{k,k+1} = N - 1$, and the diagonal elements become $-k$. So we reproduced the matrix NY_k in Eq. 70. The charges NY_k lie on the root lattice spanned by the H_{ll+1}.

Appendix B

The derivation of Eq. 34 is based on simple properties of the quantum-mechanical SU(N) rotator in an external field. We reproduce it here in a form that should render its origins clear.

We are interested in the Wilson line between two points $x(s_1)$ and $x(s_2)$, the line between the two points being parametrized by s. The line is the ordered product (from right to left) in some irreducible representation R_0 with highest weight H^0 of unitary matrices with dimension d_{R_0}:

$$W(s_f, s_i) = P \ \exp\left[ig \int_{s_i}^{s_f} A_s ds\right]. \quad (72)$$

Here $A_s = \frac{d\vec{x}}{ds}.\vec{A}$ the projection of $\vec{A}$ on the line.

The Wilson loop is covariantly constant along the curve L, $\partial_s W^\dagger(s, s_i) - igW^\dagger A_s = 0$, so along the loop one can write the vector potential as a pure gauge

$$A_s = \frac{-1}{ig} U \partial_s U^\dagger \quad (73)$$

with $U = W(s, s_i)U_i$ with U_i an arbitrary SU(N) matrix. So the loop becomes in the representation R_0 the unitary matrix :

$$D^{R_0}(U_f U_i^\dagger). \quad (74)$$

We close the Wilson loop (so s_f and s_i represent the same point) and take the trace of Eq. 74. The main result of this appendix is:

- The sum over all irreducible representations of the normalized trace of the Wilson loop is the group average of the propagator of the SU(N) rotator with Hamiltonian $\mathcal{H}$ in the external field H^0, Eq. 82.

- Then a special limit of the path integral version of this propagator, Eq. 86, is nothing but Eq. 34.

To define the Hamiltonian we start with the generators l_a of the group SU(N). They act as left multiplication on the Hilbert space defined on the group manifold, with kets $|U\rangle$, U an SU(N) element. The generators obey the commutation relations

$$[l_a, l_b] = i f_{abc} l_c, \quad \text{with} \quad f_{abc} f_{a'bc} = N \delta_{aa'}. \tag{75}$$

The $N-1$ diagonal generators l_d are denoted by the suffix d, whereas a general generator is denoted by indices a.

Likewise we can define the generators r_a of right multiplication.

The state space of kets $|\Omega>$ is has an complete orthogonal basis consisting of all the irreducible representations $D^R(\Omega)_{l,r}$, and the orthogonality relations read:

$$\int d\Omega \; D^R_{k,l}(\Omega) D^{R'}_{m,n}(\Omega^\dagger) = \frac{1}{d_{R_0}} \delta_{R,R'} \delta_{k,n} \delta_{l,m}. \tag{76}$$

The dimension of the representation R equals $\mathrm{Tr}\{D^R(\mathbf{1})\} = d_R$. We define kets and bras $|R; l, r\rangle$ with the property:

$$\langle \Omega | R; l, r \rangle = D^R(\Omega)_{l,r}. \tag{77}$$

From Eq. 76 one sees that the norm of such kets is d_R^{-1}.

The Hamiltonian is defined in terms of the left multiplication generators as:

$$\mathcal{H} = \frac{1}{2I} \Big(\sum_a l_a^2 - \sum_d l_d^2 + \sum_d (l_d - \frac{1}{2} H_d^0)^2 \Big). \tag{78}$$

The last term represents the coupling of the rotator to the highest weight H^0 written in component form $H_0 = \sum_d H_d^0 \frac{\lambda_d}{2}$, which gives a Zeeman effect for the energy levels in any representation R.

Write $\sum_a l_a^2 = C_2(R)$ for the value of the quadratic Casimir in R and denote l for the $N-1$ diagonal quantum numbers l_d in $D(\Omega)_{l,r}$. Similarly the $N-1$ diagonal right multiplication generators have quantum numbers, denoted by r. Then one has for the eigenvalues E^0 of this Hamiltonian:

$$E^0(R, l) = \frac{1}{2I} (C_2(R) - \sum_d l_d^2) + \frac{1}{2I} \sum_d (l_d - \frac{1}{2} H_d^0)^2. \tag{79}$$

Let us find the corresponding Lagrangian L . Define the angular velocities from the special unitary matrices S:

$$V_a = i \; \mathrm{Tr}\, \{ S \partial_s S^\dagger \lambda_a \}. \tag{80}$$

Then:

$$L = \frac{I}{2} \sum_a V_a^2 + \frac{1}{2} \sum_d V_d H_d^0. \tag{81}$$

This Lagrangian gives the Hamiltonian in terms of the canonical momenta $J_a = \frac{\partial L}{\partial V_a}$. There is a subtlety: upon quantization we have the generators of left and right SU(N) rotations, related by the adjoint representation. The question is then to which the J's do correspond. This question is only relevant for the linear term,since the quadratic term is invariant under the adjoint. A short calculation shows that the left generators correspond to the J's.

Let us now prove the following relation between the characters of the group and the integrated propagator of the SU(N) symmetric top:

$$\begin{aligned} & \int d\Omega \ \langle \Omega U_f | \exp\left\{ i(s_f - s_i)\mathcal{H} \right\} | \Omega U_i \rangle \\ = & \sum_{R,l} \mathrm{Tr}\left\{ D^R(U_f U_i^\dagger) \right\} \ \exp\left[i(s_f - s_i) E^0(R,l) \right]. \end{aligned} \tag{82}$$

On the r.h.s. we integrate over SU(N) matrices Ω, with the measure normalized to 1.

To prove this, insert the set of intermediate states $|R;l,r>$ from Eq. 77 into the l.h.s. :

$$\begin{aligned} & \int d\Omega \ \langle \Omega U_f | \exp\left\{ i(s_f - s_i)\mathcal{H} \right\} | \Omega U_i \rangle \\ = & \int d\Omega \sum_{R,l,r} d_R \ \langle \Omega U_f | R;l,r \rangle \ \exp\left[i(s_f - s_i) E^0(R,l) \right] \ \langle R;l,r | \Omega U_i \rangle. \end{aligned} \tag{83}$$

The right index r can be summed over, and using Eq. 77 one finds:

$$\sum_r \langle \Omega U_f | R;l,r \rangle \langle R;l,r | \Omega U_i \rangle = D^R(\Omega U_f (\Omega U_i)^\dagger)_{l,l}. \tag{84}$$

Integration over Ω gives, for fixed l, using Eq. 76:

$$\int d\Omega \ D^R(\Omega U_f (\Omega U_i)^\dagger)_{l,l} = \frac{1}{d_R} \mathrm{Tr}\left\{ D^R(U_f U_i^\dagger) \right\} \tag{85}$$

Plug this result into the r.h.s. of Eq. 83, and we have the main result Eq. 82.

Now we want to project out from the main result the representation R_0. This is done by letting $I \to 0$ in the energy exponent and determining the minimum of $E^0(R,m)$. One such minimum is realized by $\frac{1}{2} H_d^0 = m_d$ and $C_2(R) = C_2(R_0)$.

So the sum over all irreducible representations R in Eq. 82 reduces in this limit to the representation R_0 singled out by the its corresponding highest weight H^0.

Strictly speaking there is only one minimum when H_0 is the weight of the fundamental representation, or of any of the representations corresponding to a fully antisymmetric Young tableau. The reason is that for fixed $\mathcal{N}$-ality $C_2(R)$ takes its minimum value for R being fully antisymmetric.

For higher representations, like e.g. in SU(2) with weight j_0(the number of boxes in the Young tableau), there is the representation $R = j_0 - 1$, with $m = j_0 - 1$, that minimizes E^0 as well. This is why in the original work [49] the *asymmetric* top was taken, to provide an independent inertia in front of the Zeeman splitting in Eq. 79 and taking them independently to zero. So from now on the irrep R_0 stands for one of the totally antisymmetric representations.

Of course the result contains the rapidly varying phase factor

$$\exp\left[i(s_f - s_i)\frac{E^0(R_0, H_0)}{2I}\right] = \exp\left[i(s_f - s_i)\left(C_2(R_0) - \frac{1}{2}\mathrm{Tr}\left\{H_0^2\right\}\right)/2I\right] \equiv F(R_0).$$

According to appendix A the value in this minimum is $C_2(R_0) - \frac{1}{2}\mathrm{Tr}\left\{H_0^2\right\} = \sum_{l=1}^{N-1} w_l(N-l)lN$ with w_l the weights defined by the Young diagram of R_0. This same factor $F(R_0)$ appears also in front of the path integral transcription of the matrix element:

$$\langle \Omega U_f | \exp\left\{i(s_f - s_i)\mathcal{H}\right\} |\Omega U_i\rangle = F(R_0) \int_{\Omega U_f}^{\Omega U_i} DS(s)\ \exp\left[-i\int ds L\right] \tag{86}$$

with L as in Eq. 81. This formula, together with the fact that the left generators in the matrix element are correctly represented by the path integral can be proved straightforwardly. We introduce the periodic fluctuation variable $\Omega(s)$ with $\Omega(s_{i,f}) = \Omega$ and transform the fluctuation variable S in Eq. 86:

$$S(s) = \Omega(s)U(s) \qquad \text{with} \quad D\Omega = DS. \tag{87}$$

The path integral now becomes:

$$\int_{\Omega}^{\Omega} D\Omega(s)\ \exp\left[-i\int ds L\right] \tag{88}$$

with L as in Eq. 81, but with the substitution Eq. 87 in the angular velocities V_a in (80):

$$\begin{aligned} V_a &= \mathrm{Tr}\left\{\Omega(s)U(s)\partial_s(\Omega(s)U(s))^\dagger \lambda_a\right\} \\ &= \mathrm{Tr}\left\{\left(\Omega(s)(U(s)\partial_s U(s)^\dagger)\Omega(s)^\dagger + \Omega(s)\partial_s\Omega(s)^\dagger\right)\lambda_a\right\}. \end{aligned} \tag{89}$$

Finally use Eq. 73 to write the angular velocity as the gauge transformed potential A_s:

$$V_a = \mathrm{Tr}\left\{\left(\Omega(s)(-igA_s)\Omega(s)^\dagger + \Omega(s)\partial_s\Omega(s)^\dagger\right)\lambda_a\right\} = \mathrm{Tr}\left\{\left(\Omega(s)\nabla_s\Omega(s)^\dagger\right)\lambda_a\right\}. \tag{90}$$

Remember $\nabla_s\Omega(s)^\dagger = \frac{d\vec{x}}{ds}.(\vec{\partial} - ig\vec{A})\Omega(s)^\dagger$.

The final form of the Wilson loop in the irrep R_0 and with highest weight H_0 follows from Eq. 81, 82 and 86:

$$W_{R_0} = \lim_{I\to 0}\int D\Omega\ \exp\left[-i\frac{I}{2}\oint ds \sum_a V_a^2 - \oint ds\ \mathrm{Tr}\left\{H_0(\Omega\vec{\nabla}\cdot\frac{d\vec{x}}{ds}\Omega^\dagger)\right\}\right]. \tag{91}$$

The line integral on the r.h.s. can be easily transformed into a surface integral, because it now involves the gauge transform average of potential projected on the highest weight, i.e. an Abelian potential. The surface S bounded by the loop L is covered by a set of nested loops $L(r)$ with $L(r=0) = L$ and $L(r=1)$ shrunk to a point. Then, in an obvious notation:

$$\begin{aligned} & -\oint_L ds\ \mathrm{Tr}\left\{H_0(\Omega\nabla_s\Omega^\dagger)\right\} \\ = & \int_0^1 dr\ \partial_r \oint ds\ \mathrm{Tr}\left\{H_0\Omega\nabla_s\Omega^\dagger\right\} \\ = & \int_0^1 dr \oint ds\ \mathrm{Tr}\left\{H_0\left(\epsilon_{rs}\nabla_r\Omega\nabla_s\Omega^\dagger) + \epsilon_{rs}\Omega\nabla_r\nabla_s\Omega^\dagger\right)\right\} \end{aligned} \tag{92}$$

which gives then Eq. 34, using the commutator $[\nabla_r, \nabla_s] = -igF_{r,s}$. The gauge transform in the last expression is now extended to all of the surface S and beyond. This surface is of course arbitrary, apart from its boundary.

Appendix C

We give the explicit form of our Polyakov loops with $\mathcal{N}$-ality k. Let $P(x,y,t) \equiv \prod_{n=1}^{L/a} \tilde{U}_x(x+na,y,t)$, where $\tilde{U}_x(\mathbf{x})$ stands either for the original link variable $U_x(\mathbf{x})$ or a fuzzy [29] version of it with the same gauge transformation properties. Then our operators are [25]

$$\mathcal{O}^{(k)}(t) = \frac{a}{L_y} \sum_m O^{(k)}(x, y+ma, t) \tag{93}$$

where the operator $O^{(k)}$ is one of

$$k=2: \quad \frac{1}{N}\mathrm{Tr}\{P^2\} \qquad \frac{1}{N^2}(\mathrm{Tr}\{P\})^2 \tag{94}$$

$$k=3: \quad \frac{1}{N}\mathrm{Tr}\{P^3\} \qquad \frac{1}{N^3}(\mathrm{Tr}\{P\})^3 \qquad \frac{1}{N^2}\mathrm{Tr}\{P^2\}\mathrm{Tr}\{P\} \tag{95}$$

$$k=4: \quad \frac{1}{N}\mathrm{Tr}\{P^4\} \qquad \frac{1}{N^4}(\mathrm{Tr}\{P\})^4 \qquad \frac{1}{N^2}(\mathrm{Tr}\{P^2\})^2 \tag{96}$$
$$\frac{1}{N^2}\mathrm{Tr}\{P^3\}\mathrm{Tr}\{P\} \qquad \frac{1}{N^3}\mathrm{Tr}\{P^2\}(\mathrm{Tr}\{P\})^2,$$

where the argument of P is the same as that of $O^{(k)}$ in Eq. 93. The correlation functions we measure are $\langle \mathcal{O}^{(k)}(0)(\mathcal{O}^{(k)}(t))^* \rangle$.

I:$\beta = 115.0$ $V = 24 \times 28 \times 24$	$k = 1$	$k = 2$	$k = 3$	$k = 4$
$L = 24$	1.536(19)	2.67(13)	/	/

II:$\beta = 115.0$ $V = 16 \times 20 \times 24$	$k = 1$	$k = 2$	$k = 3$	$k = 4$
$L = 16$	1.0075(31)*	1.729(30)	2.216(66)	2.32(12)
$L = 20$	1.2787(33)*	2.174(59)	2.55(23)	3.04(33)

III:$\beta = 115.0$ $V = 12 \times 16 \times 24$	$k = 1$	$k = 2$	$k = 3$	$k = 4$
$L = 12$	0.7338(38)*	1.275(24)	1.680(27)	1.789(36)
$L = 16$	0.9980(45)*	1.702(28)	2.157(52)	2.423(93)

IV: $\beta = 138.0$ $V = 20 \times 24 \times 24$	$k = 1$	$k = 2$	$k = 3$	$k = 4$
$L = 20$	0.808(10)	1.436(15)	1.826(20)	1.985(29)
$L = 24$	0.991(13)	1.745(20)	2.214(42)	2.28(11)

V: $\beta = 138.0$ $V = 16 \times 20 \times 24$	$k = 1$	$k = 2$	$k = 3$	$k = 4$
$L = 16$	0.6348(58)	1.1580(96)	1.464(12)	1.540(15)
$L = 20$	0.8253(75)	1.462(15)	1.845(19)	1.937(29)

VI:$\beta = 172.5$ $V = 24 \times 28 \times 36$	$k = 1$	$k = 2$	$k = 3$	$k = 4$
$L = 24$	0.5869(32)	1.0260(82)	1.303(18)	1.401(19)
$L = 28$	0.6961(58)	1.242(12)	1.564(34)	1.576(57)

VII:$\beta = 172.5$ $V = 20 \times 24 \times 36$	$k = 1$	$k = 2$	$k = 3$	$k = 4$
$L = 20$	0.4883(31)	0.8939(65)	1.109(12)	1.213(18)
$L = 24$	0.5878(43)	1.042(16)	1.308(23)	1.381(22)

Table 1: The masses of flux-tubes of different $\mathcal{N}$-alities. Values followed by a * were extracted from simulations employing a one-level algorithm. In addition, a $\beta = 138$ run on a $32 \times 32 \times 36$ lattice was done with $am_{k=1} = 1.3347(49)$ and $am_{k=2} = 2.326(49)$.

	$\beta = 115.0$	$\beta = 138.0$	$\beta = 172.5$
$a\sqrt{\sigma_1}$	0.2558(6)	0.2059(6)	0.1582(12)
γ_1	0.624(78)	0.67(12)	0.27(19)
$\sigma_2/\sigma_1\|_{L=\infty}$	1.690(52)	1.709(37)	1.695(45)
$\sigma_3/\sigma_1\|_{L=\infty}$	2.01(12)	2.162(72)	2.175(88)
$\sigma_4/\sigma_1\|_{L=\infty}$	2.28(20)	2.31(11)	2.08(12)

Table 2: Top: the fundamental string tension and the string correction coefficient (to be compared with the bosonic string value $\gamma_b = \pi/6 \simeq 0.5236$. Bottom: the ratios of k-torelon masses, extrapolated to $L = \infty$ assuming $1/L^2$ corrections at three different lattice spacings. The continuum limit $a \to 0$ of these ratios are given in section 6.2.3.

$\beta = 115.0$	$k = 2$	$k = 3$	$k = 4$
$L = 12$	1.694(33)	2.213(36)	2.352(49)
$L = 16$	1.688(28)	2.141(51)	2.319(91)
$L = 20$	1.686(46)	1.98(18)	2.35(26)
$L = 24$	1.728(84)	/	/
Mean	1.692(28)	2.184(36)	2.349(49)

$\beta = 138.0$	$k = 2$	$k = 3$	$k = 4$
$L = 16$	1.782(22)	2.239(28)	2.352(32)
$L = 20$	1.749(24)	2.208(31)	2.356(42)
$L = 24$	1.744(30)	2.207(51)	2.27(11)
$L = 32$	1.734(37)		
Mean	1.744(24)*	2.222(28)	2.349(32)

$\beta = 172.5$	$k = 2$	$k = 3$	$k = 4$
$L = 20$	1.786(18)	2.202(28)	2.404(44)
$L = 24$	1.732(17)	2.177(33)	2.317(35)
$L = 28$	1.763(23)	2.195(28)	2.230(84)
Mean	1.743(17)*	2.195(28)	2.304(35)*

Table 3: The effective ratios of k-string tensions, corrected for finite-length effects assuming Eq. (61) with bosonic string coefficient; at three different lattice spacings. The values at different L are fitted by a constant to give the 'mean' value. The mean values were obtained by averaging values at all L, except for those appearing with an asterisk *, where the shortest torelon was dropped. The continuum limit $a \to 0$ of these ratios are given in section 6.2.3.

	$m^*_{k=2}$	$\frac{1}{2}(m_{k=2}+m^*_{k=2})$	$2m_{k=1}$
II: $L=16$	2.122(60)	1.932(33)	2.015(6)
$L=20$	2.49(25)	2.33(13)	2.557(6)
III: $L=12$	1.677(37)	1.476(23)	1.468(4)
$L=16$	2.244(75)	1.973(42)	1.996(9)
IV: $L=20$	1.886(24)	1.661(17)	1.62(2)
$L=24$	2.245(59)	1.995(31)	1.981(3)
V: $L=16$	1.380(39)	1.272(23)	1.27(1)
$L=20$	1.72(10)	1.598(54)	1.65(2)
VI: $L=24$	1.328(15)	1.181(9)	1.174(6)
$L=28$	1.672(31)	1.457(16)	1.39(1)
VII: $L=20$	1.109(28)	1.002(14)	0.977(6)
$L=24$	1.296(22)	1.174(10)	1.176(8)

Table 4: The first-excited $k=2$ torelon mass. The roman numbers refer to the different runs whose parameters are given in Tab. 1.

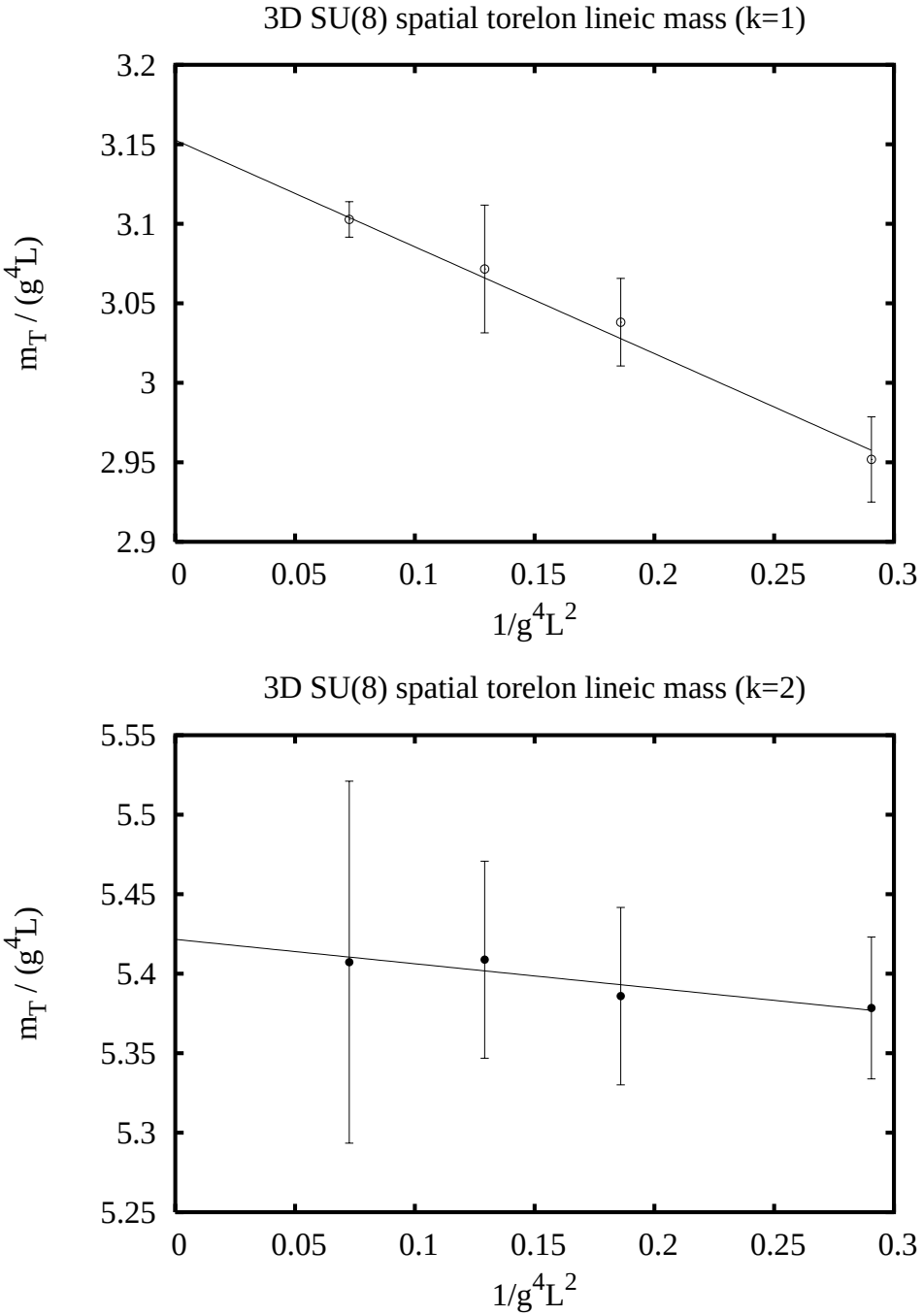

Figure 4: The lineic mass of spatial torelons in the $k = 1$ and $k = 2$ sectors at $\beta = 138$. The intercept on the vertical axis yields the string tension.

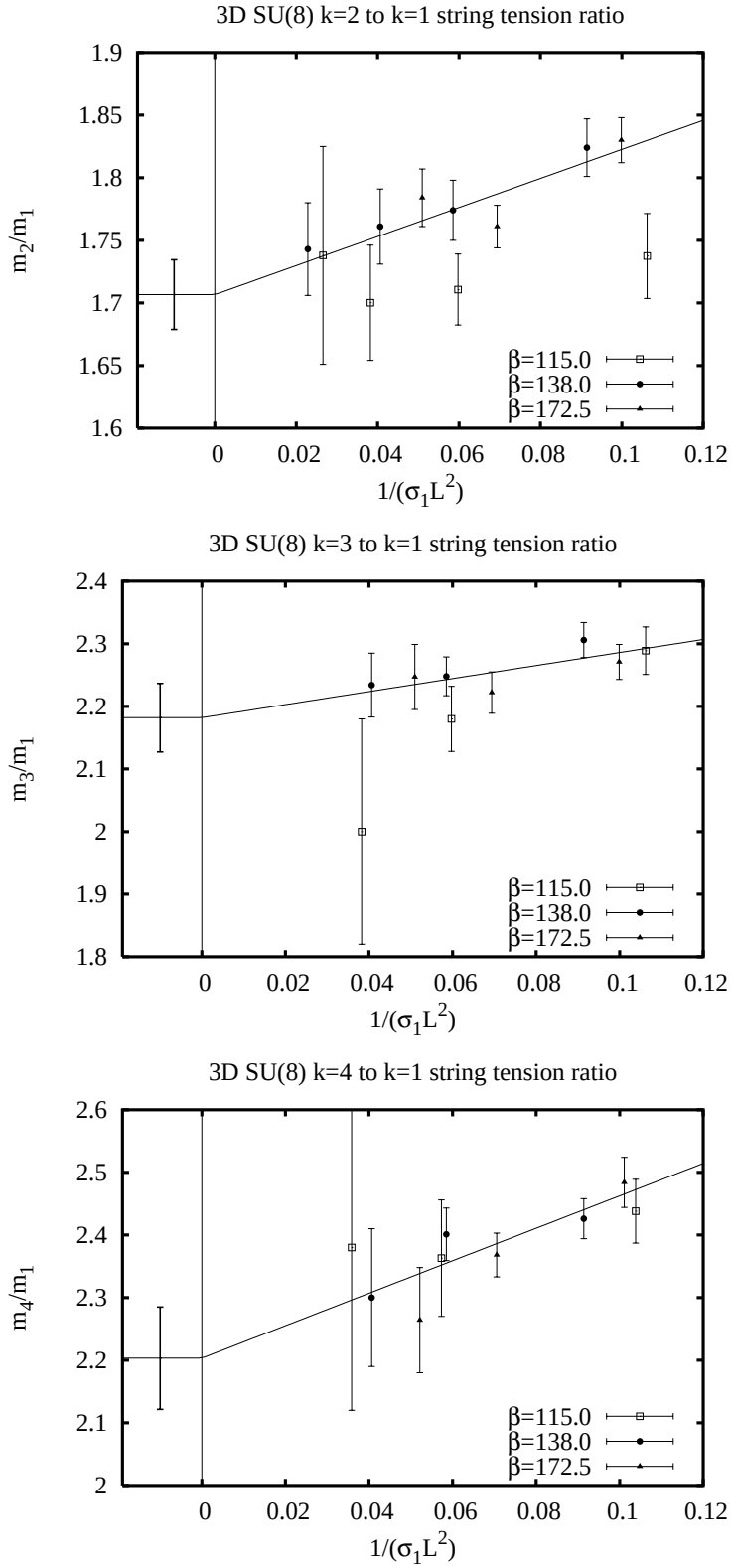

Figure 5: Final analysis: the extrapolation of the string tension ratios to infinite string length (only the filled points are included in the extrapolation). The result of the extrapolation is shown beyond the vertical axis.

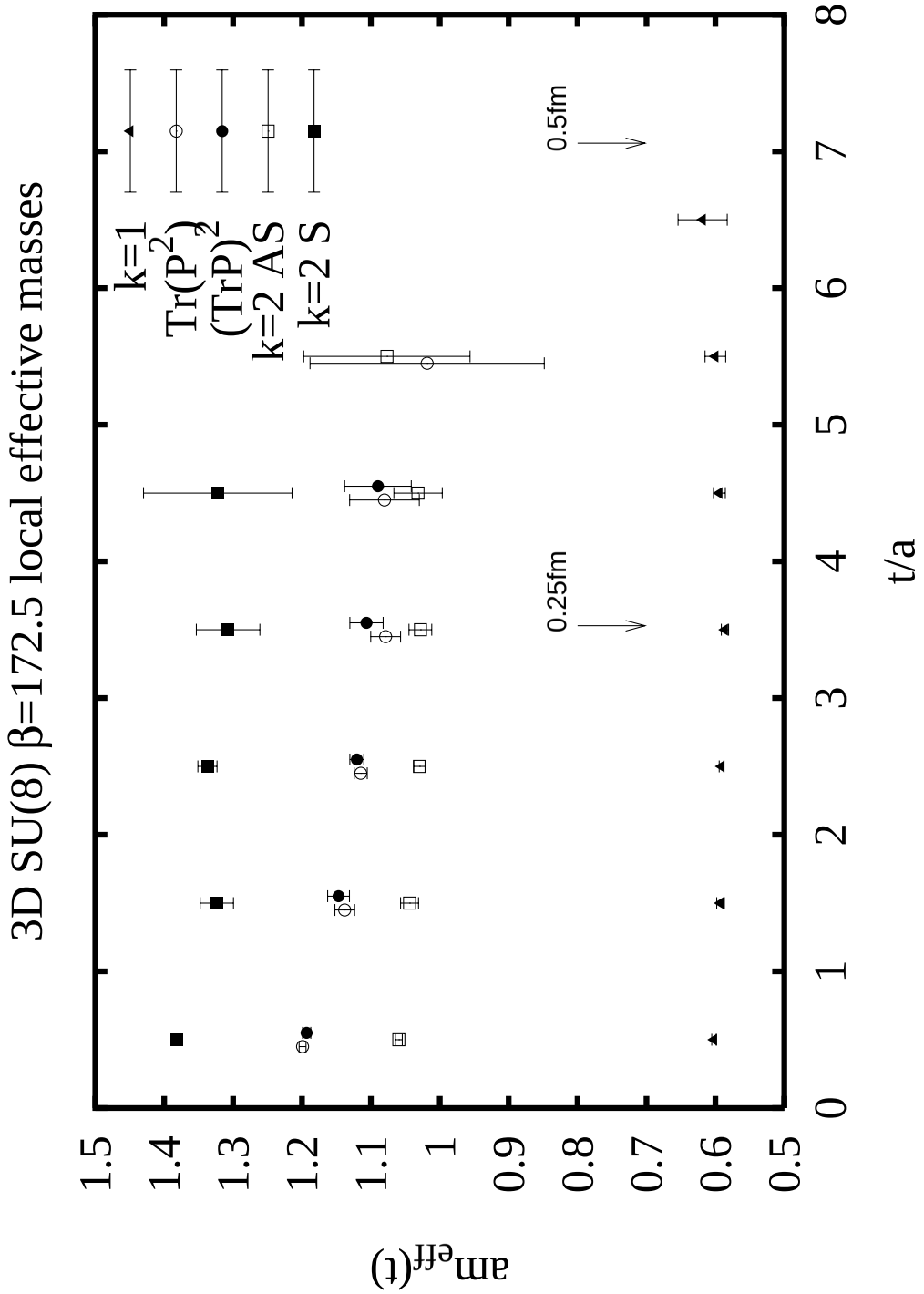

Figure 6: The local effective mass $am_{\rm eff}(t+\frac{a}{2}) \equiv \log\left(\frac{C(t)}{Ct+a)}\right)$ for the $L = 24$ k=1 and k=2 strings. The transverse dimension is $L = 28$.

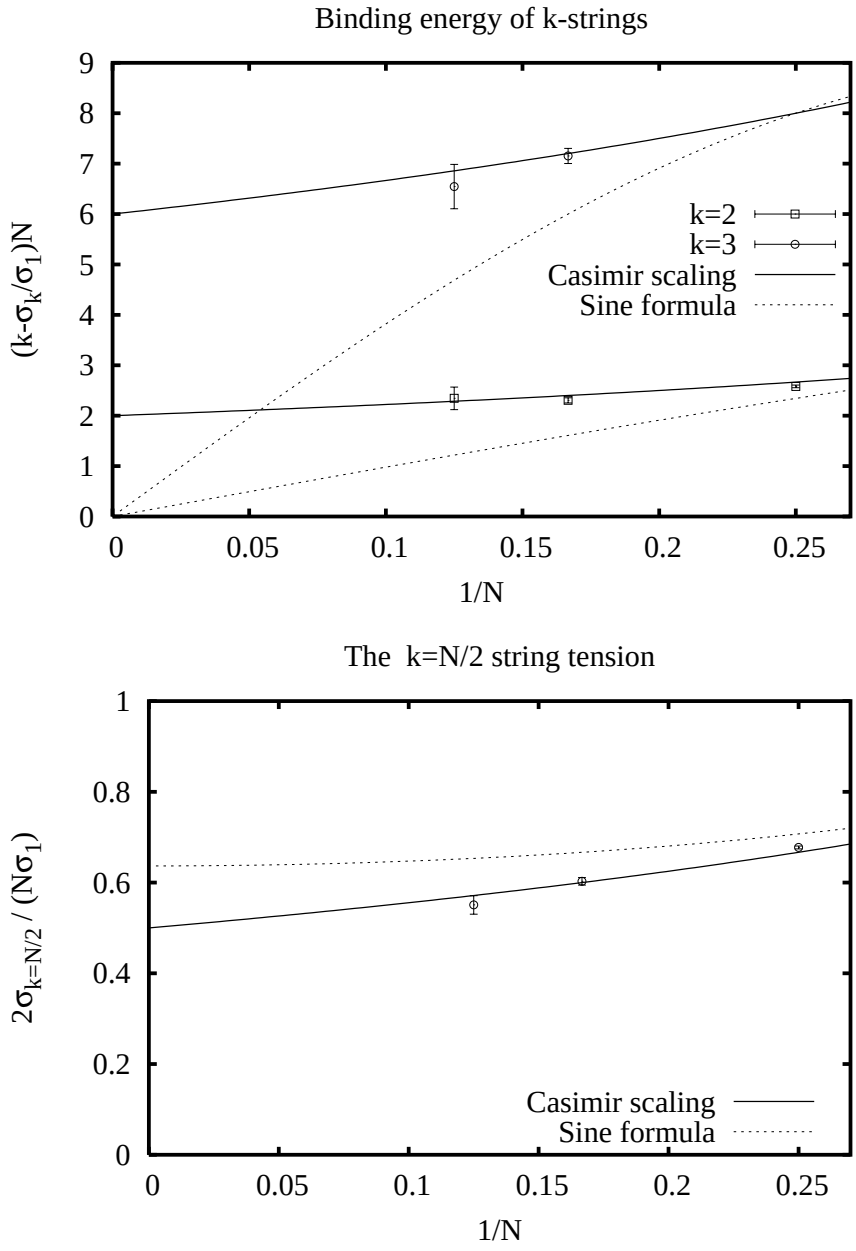

Figure 7: Top: the binding energy of k-strings per unit length, in units of σ_1 and rescaled by a factor N, as a function of N. Bottom: the string tension ratio $\frac{\sigma_{k=N/2}}{\sigma_1}$, rescaled by a factor $\frac{2}{N}$. The lattice data for SU(4) and SU(6) is taken from[25].